UNIVERSITY OF OKLAHOMA

GRADUATE COLLEGE

ESTIMATING WAVE REDUCTION BY FLOATING-WETLAND BREAKWATERS USING SMALL-SCALE PHYSICAL MODELS

A THESIS

SUBMITTED TO THE GRADUATE FACULTY

in partial fulfillment of the requirements for the

Degree of

MASTER OF SCIENCE IN ENVIRONMENTAL ENGINEERING

By

SALIOU DIALLO

Norman, Oklahoma

2020

ESTIMATING WAVE REDUCTION BY FLOATING-WETLAND BREAKWATERS USING SMALL SCALE PHYSICAL MODELS

A THESIS APPROVED FOR THE

SCHOOL OF CIVIL ENGINEERING & ENVIRONMENTAL SCIENCE

BY THE COMMITTEE CONSISTING OF

Dr. Jason R. Vogel, Chair

Dr. Keith A. Strevett

Dr. Randall L. Kolar

© Copyright by SALIOU DIALLO 2020

All Rights Reserved

Table of Contents

Table of Figures

List of Tables

Abstract

Wind-induced waves can cause significant erosion on lake shorelines. One solution to this problem is to absorb the waves before they reach the shoreline. Floating breakwaters have been used to reduce waves, but provide limited ecological benefit. On the other hand, floating wetlands have been used to improve water quality and habitat. The goal of this study is to use scale models estimate the wave height and energy reduction of floating wetlands used as breakwaters. The floating-wetland breakwaters used in this study consist of a base frame filled with Poly-flo filter material, and a cross section made of pipes of uniform diameter. The hypothesis of this study is that wave reduction results from small-scale floating-wetland breakwaters can predict the wave reduction performance of full-scale floating-wetland breakwater designs. Floating-wetland breakwater models were constructed using Froude number similitude. Wave height and energy reduction experiments were conducted on floating-wetland breakwaters at two different scales. Results indicate that, in most instances, floating-wetland breakwaters at different scales exhibit a similar wave reduction performance. Overall, this study provides a framework for individuals and agencies to design and evaluate floating-wetland breakwaters, and helps to address shoreline erosion problems in a cost-effective manner.

Chapter 1 - Introduction

Lakes and reservoirs are subject to water waves due to wind and wake action. These waves transfer energy that erodes and transports bank soil. This erosion affects ecosystems by reducing viable habitat on shorelines and banks, decreasing species diversity, and impacting water quality within the reservoir. As a result, there is a need for ways to reduce wave action in water bodies before they reach the shoreline. Floating breakwaters have been extensively used to reduce wave size and floating wetlands have mostly been used to improve water quality. Using floating wetlands as breakwaters grants the benefits from both systems. This project aims to estimate and compare the wave reduction performance of floating-wetland breakwaters (hereafter referred to as FWBs) at different scales to improve design and testing guidance and allow for testing a design as a small (lab) scale and allow for implementation at the large (reservoir) scale.

Chapter 2 - Literature Review

Coastal systems, lakes and reservoirs are subject to shoreline erosion. Breakwaters have been utilized in these systems for wave reduction, and floating wetlands have been utilized for water quality and habitat improvements. FWBs can potentially be used to provide all of these benefits. Performing a similitude study on FWBs can determine how they would perform when designed for different scales.

2.1 Shoreline Erosion

“Erosion is the geological process in which earthen materials are worn away and transported by natural forces such as wind or water” (Society NG., 2018). While this process occurs in various places, shoreline erosion has been a serious concern in lakes and other water bodies. Marani et

al. (2011) used observations and dimensional analysis to determine that the erosion rate of marsh edges was directly proportional to wave power. Leonardi et al. (2015) used data from eight different sites in the United States, Italy and Australia, and found a linear positive relationship between wave power and erosion rate in salt marshes. Ozeren and Wren (2018) performed a wave erosion analysis on cohesive and non-cohesive embankments, and concluded that both embankments eroded at a similar rate due to wave action. Water waves are often a function of the wind speed and direction (Kinsman, 2002; Sayah et al., 2005). In large reservoirs, there is enough space for wind to gradually form bigger waves that hit the shore with relatively high energy. This accentuates the erosion process of the shore. For natural systems that are not heavily destabilized, reducing the forcing function of the waves can reduce the erosion of the shoreline.

The negative effects of shoreline erosion on local ecosystems include loss of property, water quality issues from the soils eroding into the lake, loss of shoreline access for recreation, and habitat destruction for fisheries and wildlife (Allen, 2001). Sadeghian et al. (2017) states that the accumulation of sediment in a reservoir decreases the storage capacity and lifespan of the reservoir. In addition, the trapping of sediment in a reservoir reduces the sediment load downstream which can result in changes in the downstream channel pattern and enhanced coastal erosion. A study on the effects of ship-induced waves found that propwash from commercial vessel passages causes a disturbance in channel sediment which increased turbidity and suspended sediment concentrations, and reduced the presence of benthic organisms on the channel bed (Hochstein, 1986).

2. 2 Breakwaters

2.2.1 Bottom-Mounted Breakwaters

Breakwaters are structures that have been widely used to dissipate wave energy and protect shorelines. They are common in harbors and come in different forms. The main types of bottom-mounted breakwaters are: conventional rubble mound breakwater, rubble mound breakwater with monolithic crown wall, berm or S-slope breakwater and caisson-type breakwater (The Rock Manual, 2007). These breakwater designs are shown in Figure 1. Conventional rubble mound breakwaters have a trapezoidal cross section with an armour layer. They are preferred in locations where the water depth is less than 15 m because they require much more material as the depth increases. Conventional rubble mound breakwaters with crown walls are mainly used for port protection. They allow access to the breakwater which facilitates port operations and maintenance. For berm breakwaters, the armourstone is placed in a berm on the seaward slope. The armourstone, the rock used for wave protection, is allowed to move to a certain extent during severe storm events to form a stable profile. Low-crested breakwaters are used for protection in areas where overtopping is acceptable. They are usually built when aesthetics are considered and can be partially emergent or fully submerged. Caisson-type breakwaters are rubble mound breakwaters with a caisson on top of the mound. These are mainly used for port protection and are less expensive than conventional rubble mound breakwaters in water depths above 15 m. Finally, horizontally composite breakwaters are rubble mound breakwaters with a caisson behind the mound. These types of breakwaters are built on the seafloor and may be connected to the shore. Bottom-mounted breakwaters require relatively large quantities of material and are often not aesthetically pleasing. As a result, these types of breakwaters are mainly used in ports and harbors where the safety of local workers is of great concern. Another

type of breakwater is the floating breakwater which is not connected to the ground except by anchors.

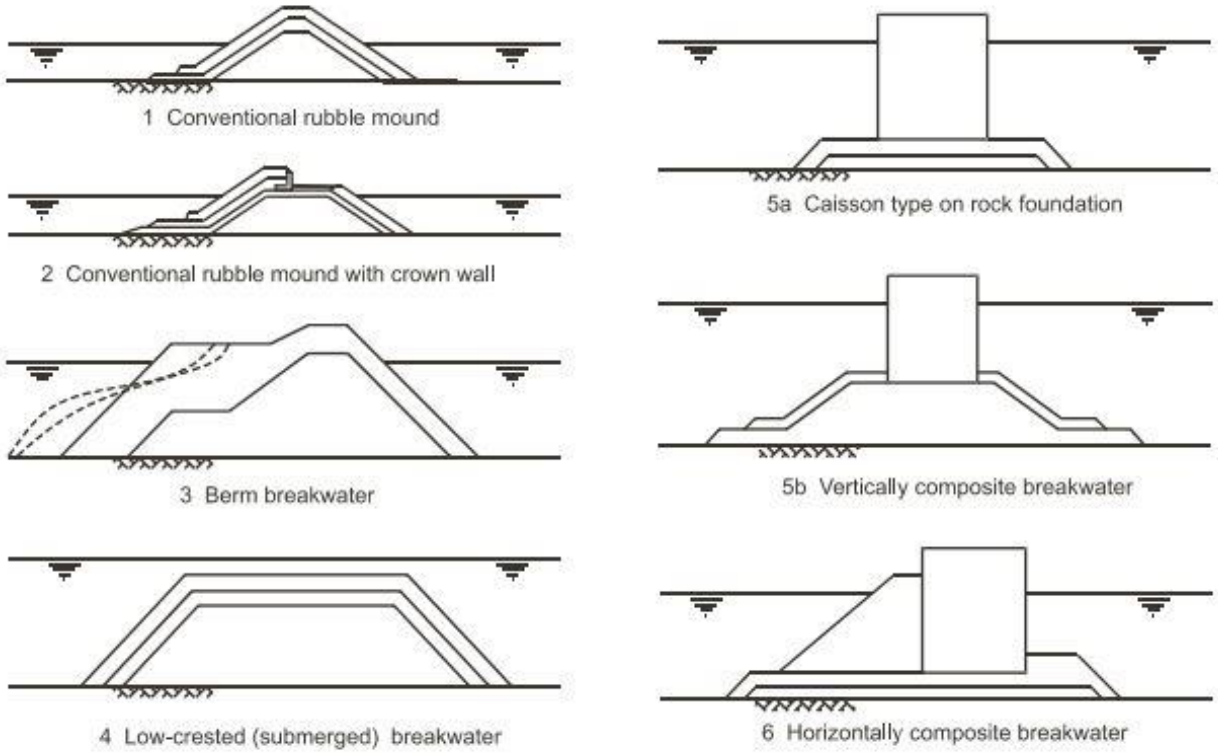

Figure 1: Different types of bottom-mounted breakwaters (The Rock Manual, 2007)

2.2.2 Floating Breakwaters

Floating breakwaters are floating structures that are designed to absorb waves. The main design of floating breakwaters is the pontoon floating breakwater which is a slab of metal or concrete that is often moored to the floor of the water body. Floating breakwaters are often restricted to relatively calm and shallow water areas, as they are structurally weaker than bottom-mounted breakwaters (Uzaki et al., 2011). The advantage of floating breakwaters is that they are adaptable to fluctuations in water level, are mobile and easily relocated, are independent of the condition of

bottom sediment, and offer less obstruction to water circulation and fish movement. Uzaki et al. used a pontoon floating breakwater with a truss in their analysis and found wave transmission coefficients (the ratio of transmitted wave height to the incident wave height) ranging from 0.1 to 1.0, depending on the ratio of water depth to wavelength. Mani (1991) and Neelamani (2018) experimented on breakwaters with a skirt wall. Neelamani determined that the addition of skirt walls improved wave reduction, which in turn decreased the required width of a floating breakwater. One drawback of using floating breakwaters is that they offer little habitat. Floating breakwaters are often constructed using concrete or steel and do not provide services to the ecosystem they are in, other than wave reduction.

2.3 Floating Wetlands

Floating wetlands are usually made of a simple slab of porous media or a buoyant mat floating in a body of water in which aquatic vegetation is established is (Pavlineri, 2017). The plant roots grow into the porous media and eventually hang down into the water column. Floating wetlands are useful in sustaining life as they can accommodate plants and animals. Also, they are widely used to improve water quality. The plants uptake nutrients such as nitrogen and phosphorus contained in the water for growth. A study by Baldy et al. (2015) found that plants reduced water phosphorus per gram of initial plant dry mass levels from 500 to 30 ug/L*g_{iDM} in the summer. Not only can this improve the trophic status of a reservoir, but it helps the plants build biomass as well. In turn, thriving plants photosynthesize and provide oxygen. Lynch et al. (2015) investigated floating treatment wetlands and found a variety of floating wetland technologies designed for nutrient remediation of stormwater. Floating wetlands can also become a viable habitat structure for aquatic, amphibian and insect species. The typical buoyant mat design of

floating wetlands is reminiscent of pontoon floating breakwaters. Floating wetlands also provide some wave reduction although that reduction has yet to be quantified.

2.4 Floating-Wetland Breakwaters

Floating breakwaters and floating wetlands are both useful in lake preservation. In systems where wave reduction is necessary but aesthetics and ecosystem services are also of concern, a FWB hybrid could be a good solution. Using floating wetlands as breakwaters is a relatively recent concept that lacks data. Martin Ecosystems (2017) has developed a floating wetland design that would also work as a breakwater. However, there is a lack of data and information on the implementation of floating wetlands as breakwaters. Webb (2014) tested the performance of the Martin Ecosystems BioHaven® Floating Breakwater. Webb found that wave transmission coefficients ranged between 0.44 and 0.99.

2.5 Similitude

The goal of any experiment is to make the results as widely applicable as possible. To achieve this end, the concept of similitude is often used so that measurements made on a system at one scale, in the laboratory for example, can be used to describe the behavior of other similar systems outside the laboratory at a larger scale (Young et al., 2007). The relationship between the model and the system must be established. In engineering, a model is a representation of a physical system that may be used to predict the behavior of the system in some desired respect. The physical system for which the predictions are to be made is called the prototype. With the successful development of a valid model, it is possible to predict the behavior of the prototype under a certain set of conditions. Construction of a successful model is accompanied by an analysis of the conditions it is tested under. Similitude is achieved when there is geometric, kinematic and dynamic similarity between the model and the prototype. A model and prototype

are geometrically similar if they are the same shape and all body dimensions in all three coordinates have the same linear-scale ratios. For kinematic similarity, the time rate of change motions of the fluid flow must be the same in the model and the prototype. Dynamic similarity is reached when all the forces acting on the system are in a constant ratio for both scales. Flow conditions for a model test are completely similar if all relevant dimensionless parameters have the same corresponding values for model and prototype. Complete similitude is often not possible; therefore, scaling is usually implemented using the most important dimensionless parameter (Stern, 2013). For systems involving free surface flow such as flow around a ship or across FWBs, the Froude number is the important similarity parameter. The Froude number is a dimensionless number defined as the ratio of inertial forces to gravitational forces. For free surface flow systems, similitude can be conducted based on an equality of Froude numbers. Ozeren (2009) performed a similitude study on pontoon floating breakwaters using this method and was able to estimate the wave reduction of a specific floating breakwater design. This study found wave transmission coefficients ranging between 0.2 and 0.9. FWB

Overall, there is a gap in current research on the use of floating wetlands as wavebreaks. A broad body of knowledge on wavebreaks is present in both coastal and inland water settings. Floating wetlands have utilized for water quality and habitat improvement. However, floating breakwaters have generally not been designed with ecosystems benefits besides wave reduction as a secondary objective. A FWB has the potential for wave reduction while also providing other ecosystem benefits. Investigation of the similitude relationships associated with their performance will allow for efficient design and implementation at multiple scales and in different sizes of reservoirs.

Chapter 3 - Hypothesis and Objectives

The main hypothesis is that the wave reduction performance of FWBs can be predicted based on small-scale model results. By conducting a similitude study on FWBs at different scales, the reduction in wave height and wave-energy density may be able to be predicted for multiple scales. This will allow economical design of full-scale FWBs based on scale model testing.

The objectives of this study are:

(1) Test and compare the wave height and wave energy reduction performance of the FWB system with varying numbers and lengths of pipes at two different scales (prototype and model);

(2) Determine scaling effects on wave height and energy reduction caused by the FWBs.

Chapter 4 - Methods

Investigating the similitude of wave reduction by FWB frames was a three-step process: (1) test wave reduction on a base system at what is referred to as “prototype scale”, (2) test wave reduction on a scaled-down version, constructed at a 1:8 scale, referred to as “model scale”; and, (3) analyze the data from these experiments to determine the effect of scale on wave reduction by FWB frames.

4.1 Prototype System

To investigate wave reduction at a scale similar to the scale that would be deployed in a reservoir, a custom wave generator was installed in an artificial pond at the Aquatic Research Facility (ARF) on the University of Oklahoma campus.– Multiple runs for various configurations

of the FWBs frames were completed, and the resulting data was collected and analyzed by manual analysis of wave video next to a staff gauge.

4.1.1 Experimental Setup

The prototype FWB system was developed based on a modified Y-frame model design. The design consisted of a 10-ft by 4-ft rectangular frame made of 4-inch polyvinyl chloride (PVC) pipe. The skirt wall was also made of 4-inch PVC pipe and was attached 2 inches below the main frame. A 6-inch layer of Poly-flo filter material (Americo Manufacturing Company Inc., Acworth, GA) was placed inside the rectangular frame. The number of pipes in the skirt wall was varied between 0, 6 and 11 pipes. The length of the pipes was varied between 0.0, 1.0, 2.0 and 3.0 ft. Two FWBs adjacent to each other were fastened together on one side and positioned perpendicular to the direction of incoming waves. Figures 2, 3 and 4 below are schematics of the FWBs while Figure 5 is an image of a FWB frame.

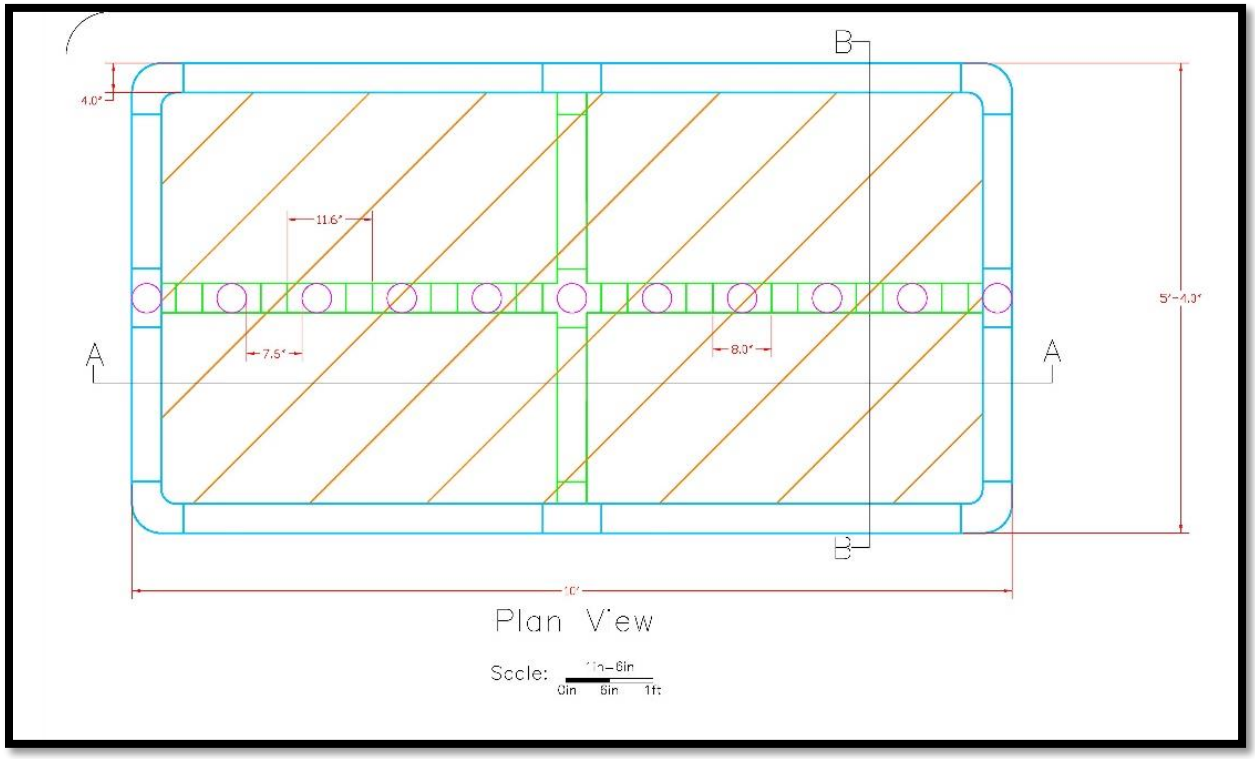

Figure 2: Top view schematic of a FWB frame. Drawing by Farzana Ahmed (OU Civil Engineering and Environmental Science).

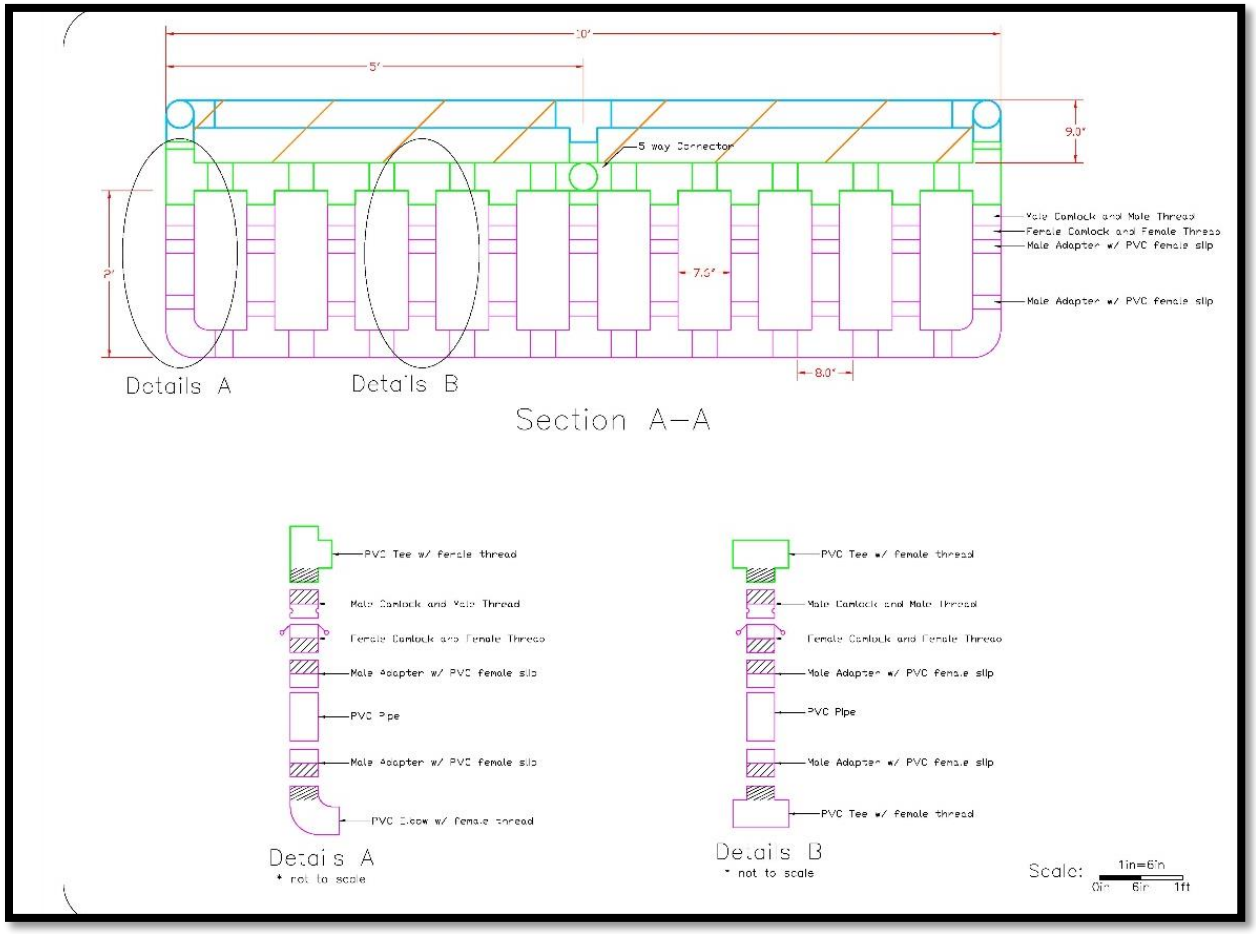

Figure 3: Section A-A' view of a FWB frame. Drawing by Farzana Ahmed (OU Civil Engineering and Environmental Science).

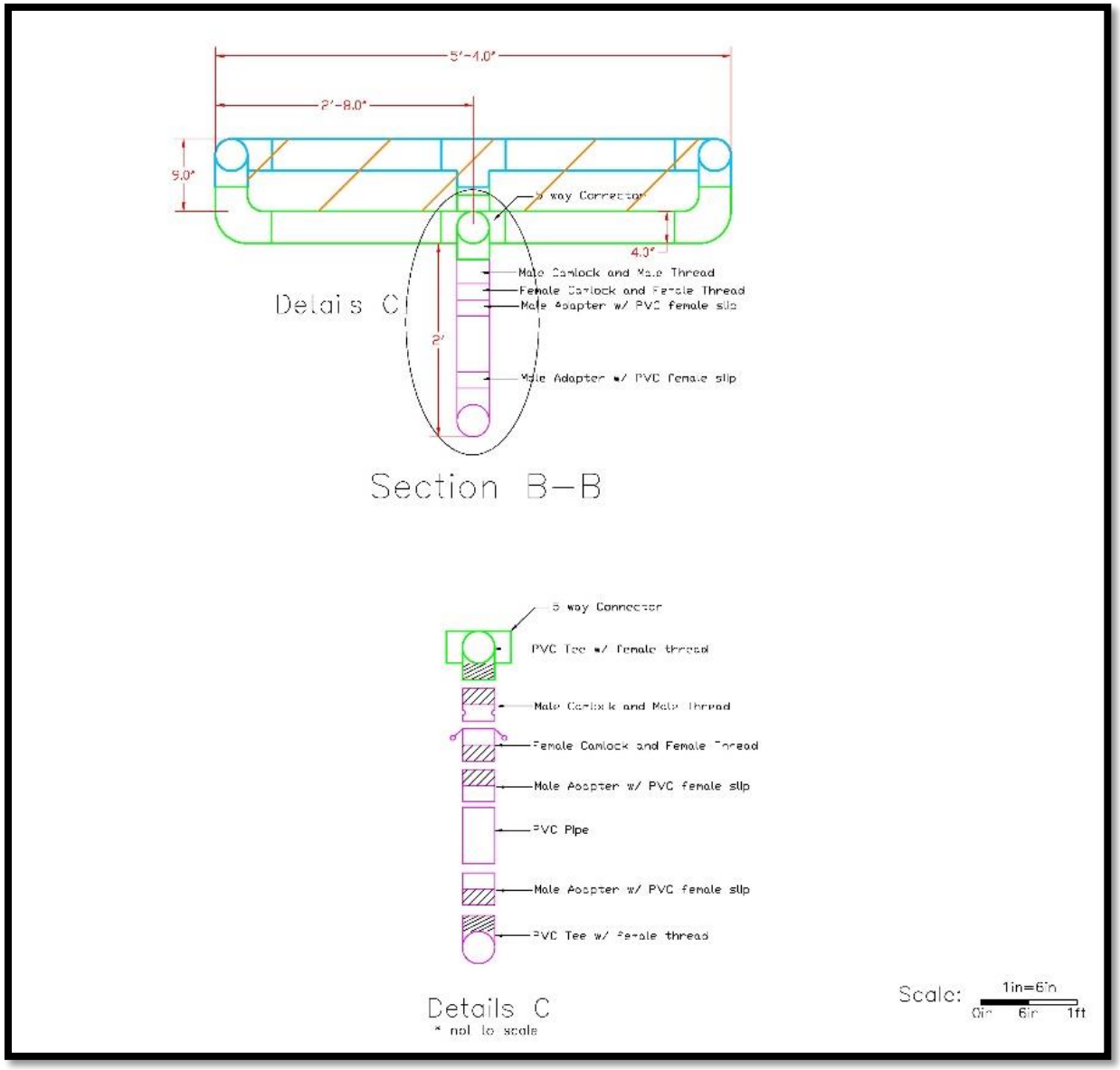

Figure 4: Section B-B' view of a FWB frame. Drawing by Farzana Ahmed (OU Civil Engineering and Environmental Science).

Figure 5: FWB frame used for prototype system (upside-down). Photo by Maxwell O'Brien (Oklahoma Water Survey)

A wave generator made waves ranging from 3 inches to 14 inches in amplitude. The wave generator, depicted in Figure 6, was comprised of paddles attached to a metal frame. The frame was connected by a metal beam to a modified tiller on the back of a John Deere 870 tractor (John Deere, Moline, IL) tractor. As the tiller rotated, the beam would push and pull the metal frame, causing the paddles to move back and forth and generate waves in the process. The rotations per minute (RPM) of the modified tiller controlled the frequency of the waves while the stroke of the modified tiller controlled the wave height. Attaching the metal beam to the outer edge of the tiller would result in a higher radius of rotation and would push the paddles farther thus

increasing the amount of water moved and the wave height. Each experimental combination of number of pipes and pipe length was subjected to different wave heights during runs. The system was maintained in deep wave conditions, which means that the depth of the water is greater than half the wavelength of the water waves (Thurman & Trujillo, 2001). The wavelength was estimated visually and determined to be smaller than double the known water depth. The depth of the water in the pond increased from the side of the wave generator to the other end. The water depth was 5 feet at the location where the FWBs were placed in the pond. Waves that travelled through the FWBs had roughly half of the pond length left to travel before reaching the end of the pond. This was done to minimize the reflection of waves which would affect the wave measurement results. Also, runs were limited to two minutes since the wave reflection usually became apparent after that time. The FWBs were anchored at the four corners using rope and cement blocks. The FWBs were sized such that minimal space was present between them and the edges of the pond. Because of the position and anchoring pattern on the FWBs, their only types of motion were pitch (up-down rotation by the transverse or side-to-side axis) and heave (linear up-down motion).

Figure 6: Wave generator used for prototype system. Photo by Maxwell O'Brien (Oklahoma Water Survey)

4.1.2 Data Collection

During runs, the wave height and period were measured in front of and behind the FWBs. To do this, staff gauges were attached to anchors and held vertically at the water surface. HERO 7 Black cameras made by GoPro (GoPro, San Mateo, CA) were attached to the meter sticks and recorded the oscillation of the water level on the meter stick during runs. Figure 7 shows the experimental setup for the base system.

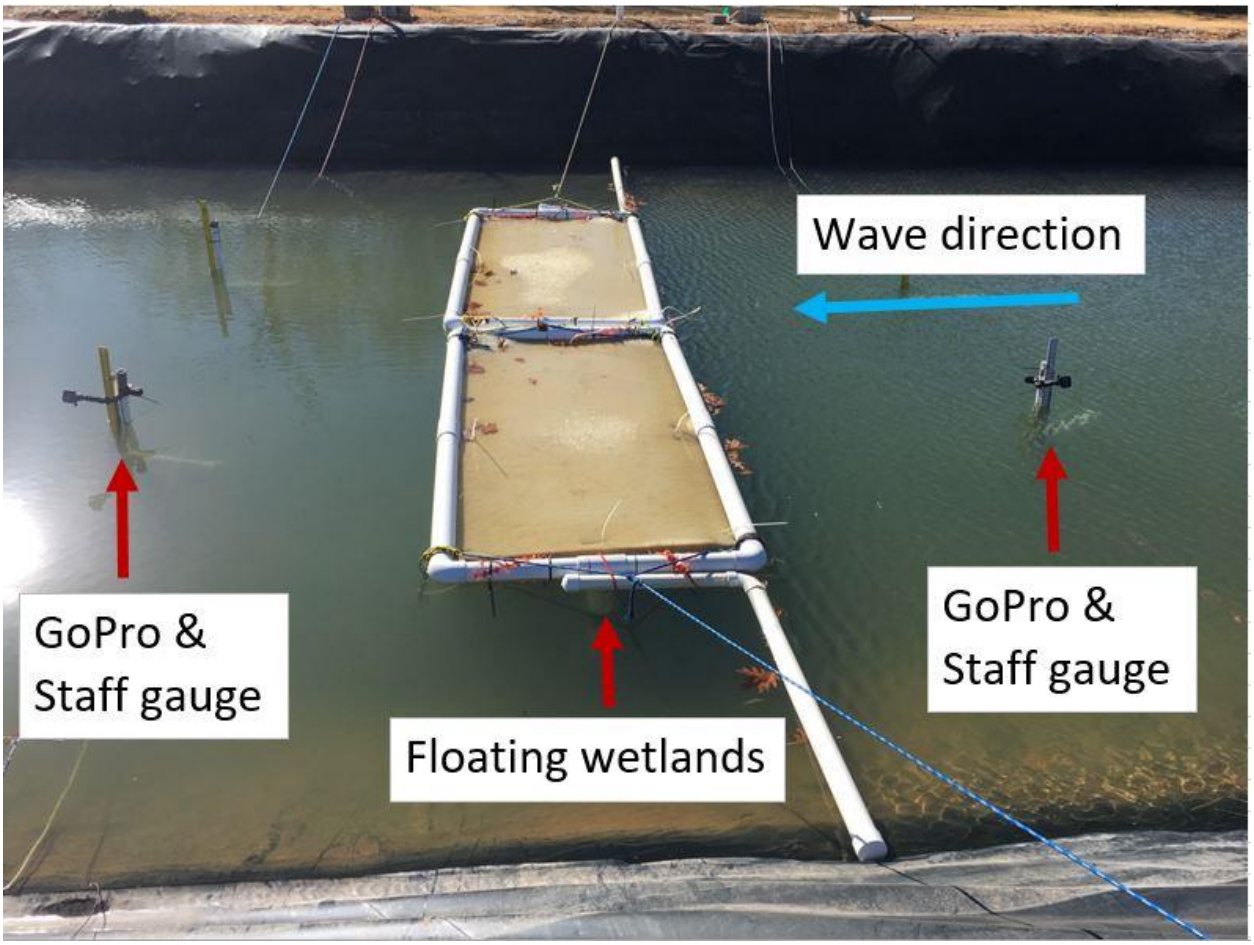

Figure 7: Experimental setup for prototype system. Photo by Maxwell O'Brien (Oklahoma Water Survey)

4.2 Scale-model System

The scale model was tested in laboratory S-22 in Carson Engineering Center at the University of Oklahoma. After properly scaling the FWBs used for the prototype using the Froude number method, the scale model was tested in a flume for waves that were manually generated. This section describes the scaling process, the testing process and the data collection methods.

4.2.1 Scaling

The Froude number was used to scale the FWB system from the prototype scale to the small scale. The Froude number is the ratio of inertial forces over gravitational forces and is denoted as

$$Fr = \frac{u}{\sqrt{gL}} \quad (1)$$

where u is the relative flow velocity

g is the acceleration due to gravity, and

L is a characteristic length, a representative length of a system such as diameter or width.

The Froude number is often used when dealing with free-surface flow systems. It is appropriate here because the FWBs are located at the surface of the water and interact with waves. In order to properly scale a free-surface system like FWBs, an equality of Froude numbers must be achieved between the prototype system and the model. This allows for proper scaling of the FWBs as well as the forces that act on them. A scale of 1:8 based on the length was chosen for the experiments. All lengths pertaining to the FWB frame, as well as wave heights were scaled by a ratio of 1:8 compared to the initial design. This resulted in FWB frames that were 7.5 in wide. The pipe lengths tested were 0.0, 1.5, 3.0 and 4.5 inches. The length of the frame did not need to be scaled exactly as long as the fraction of the cross section occupied by pipes did not change. It was assumed that the FWB is not required to be longer than the incoming waves, as long as every wave is fully intercepted by the FWB. For example, a wave measuring 6 in across hitting the center of a 12-in long FWB would be reduced the same as if it hit the center of a 24-in long FWB. The FWB model was constructed to be only slightly smaller than the flume that it was installed in such that the incoming waves would fully be intercepted by the model. On the

prototype, the outer diameter of the pipe was 4.5 in and length of the frame was 10 ft, or 120 in. This means that for 11 pipes, the fraction of the length that was obstructed by pipes in the cross section was (11*4.5 in) / 120 in = 0.41. For 6 pipes, the fraction was 0.22. At the 1:8 scale, the frames were 23.5 inches long and the pipe outer diameter was 0.84 inches which corresponds to 0.5 in PVC pipe. For the same cross-sectional area obstructed by pipes, the number of pipes were 11 and 6 pipes as shown in Figure 8.

(0.41 * 23.5 in) / 0.84 in = 11.47 = 11 pipes

(0.22 * 23.5 in) / 0.84 in = 6.15 = 6 pipes

Figure 8: FWB scale model number of pipes calculations

Since the numbers of pipes were rounded, the new fractions of length occupied by pipes and the associated error were calculated in Figure 9.

For 11 pipes: (11 * 0.84 in) / 23.5 in = 0.39

The difference was then: (0.41 – 0.39) / 0.41 * 100% = 4.7%

For 6 pipes: (6 * 0.84 in) / 23.5 in = 0.21

The difference was: (0.22 – 0.21) / 0.22 * 100% = 4.7%

Figure 9: FWB scale model calculations of error resulting from difference in numbers of pipes

For the sake of this experiment, 4.7% was deemed an acceptable level of error.

As described by LeMehaute (1976), the Froude number leads to the following relationship:

$$\left(\frac{V_m}{V_p}\right)^2 = \frac{L_m}{L_p} = \lambda \qquad (2)$$

where V is wave velocity

L is characteristic length

m refers to the scale model

p refers to the prototype or full scale

λ is the scaling ratio which is 1:8 or 0.125 in this case.

Knowing that wavelength is equal to wave velocity multiplied by wave period, rearranging Equation (2) yields the following relationship:

$$\frac{T_m}{T_p} = \frac{L_m/V_m}{L_p/V_p} = \lambda^{1}/_{2} \quad (3)$$

where T is time frame which corresponds to wave period.

By scaling the wave period in the experiments by a factor of $(1/8)^{1/2}$, the velocity and wavelength were properly scaled. The wave periods observed at the prototype scale varied between 1.3 and 2.3 seconds. As a result, the target wave periods used in the 1:8 scale experiments were between 0.46 and 0.81 seconds.

4.2.2 Experimental Setup

The experiments were conducted in a 7.0 ft x 2.0 ft x 2.0 ft flume (Figure 10). Deep-wave conditions, where the water depth is greater than half of the wavelength of the incoming waves, were maintained in all runs. The wavelength was estimated visually and determined to be smaller than double the known water depth. The FWBs were anchored with small bungee cords attached to Marshalltown 4.5-in diameter, 15-lbs blue rubber tile suction cups (Marshalltown, Marshalltown, IA) at the four corners of the frame. Experiments at both scales used this anchoring pattern. Waves were generated on one end of the flume by manually raising and lowering a piece of wood in the water at a constant pace. The waves then traveled towards the other end of the flume. Artificial plants and filter material were placed at the end of the flume to

dissipate the wave energy and prevent wave reflection. The experimental setup is shown in Figure 10.

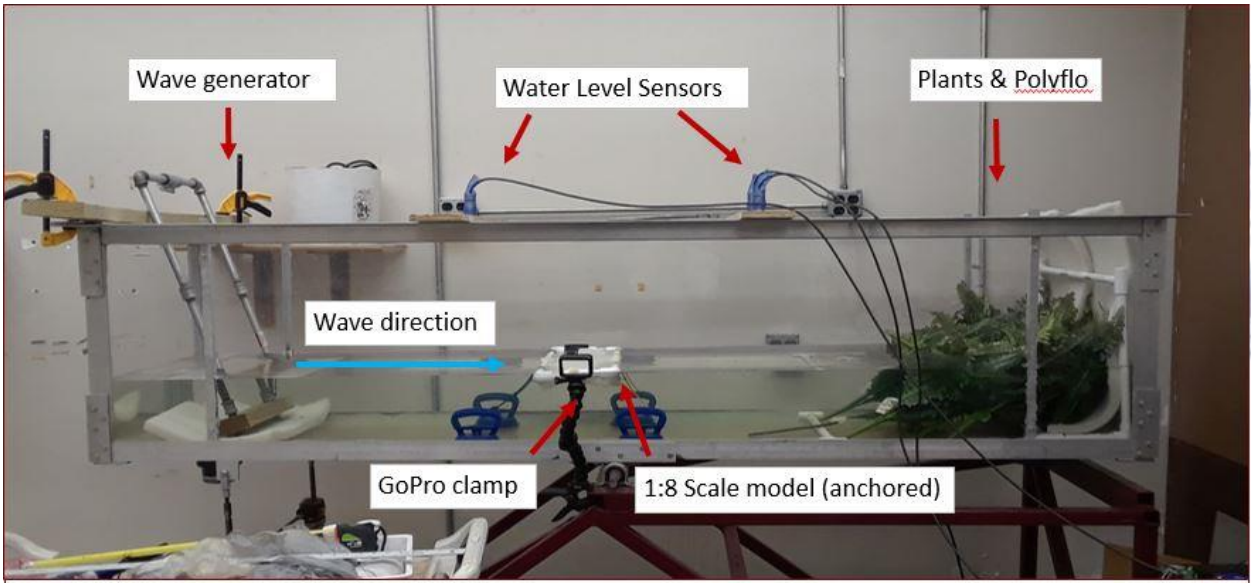

Figure 10: Experimental setup for 1:8 scale

4.2.3 Data Collection

Wave heights and periods were measured using Senix Toughsonic 3 (Senix Corporation, Hinesburg, VT) ultrasonic water-level sensors. The sensors were placed above the water surface and measured depth to water on a continuous basis. These sensors measured the wave heights in front of and behind the FWB scale model and were synchronized to take measurements at the same time. To validate the data from the ultrasonic sensors, a HERO 7 Black GoPro captured videos of selected runs. Meter sticks were placed in front of and behind the FWB so that wave peaks and troughs could be estimated on the GoPro videos and recorded in Microsoft Excel (Microsoft Corporation, Redmond, WA). Results from the GoPro videos were then compared with the data from the sensors.

4.3 Comparison of Wave Measurement Methods

Different wave measurement methods were employed over the course of the wave reduction experiments. At the 1:8 scale, ultrasonic sensors, video recording, pressure transducers and eTape water level sensors were used. These wave measurements methods and their effectiveness or lack thereof are discussed in this section.

4.3.1 Ultrasonic sensors

Ultrasonic sensors were first used because they can measure depth to water multiple times per second. This was important at the 1:8 scale because the wave period was shorter than at the prototype scale. However, the ultrasonic sensors did not store data. In order to collect data onto a computer, the sensor had to be connected to a computer. However, only one sensor could be connected at a time which made it difficult to collect data from the sensor at the front and the two at the back at the same time. As a result, a Python code was developed to collect data from multiple sensors at the same time and was used throughout the experiments on the 1:8 scale. The second problem with the data collection came from the measurements. The sensors were designed to measure depth to a smooth surface. However, the water surface was not always smooth because making waves produced turbulence and bubble formation. As a result, the ultrasonic sensors sometimes failed to estimate the depth to water. Whenever this happened, a value of 0 would be the output for that measurement. This was mostly an issue for the sensor in the front because the FWB model reduced turbulence and the waves in the back were smoother. When analyzing the wave data, Microsoft Excel was used to find local maximums and minimums as potential peaks and troughs from the waves. However, if too many 0 values were present (more than 5% of all data points), it would be difficult to determine where the peaks and troughs were as those 0 values may have in fact been peaks or troughs. Ideally, a run would at

least have a 30 second stretch with little to no 0 values to allow for proper data analysis. If there were too many 0 values, the run would not be analyzed as it could not accurately represent the wave data. Figure 11 shows an example of data that has nine 0 values in a 12 second interval. Figure 12 is the same graph on a smaller scale.

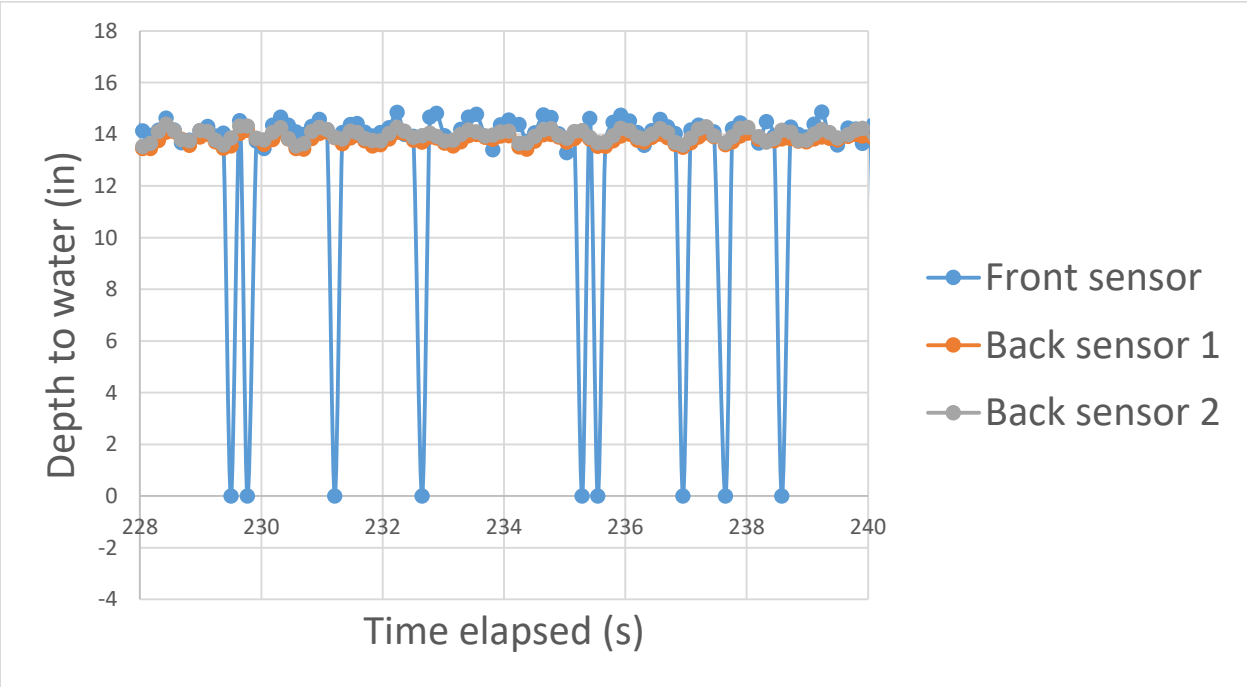

Figure 11: Example of wave measurement data including anomalous and incorrect 0 values.

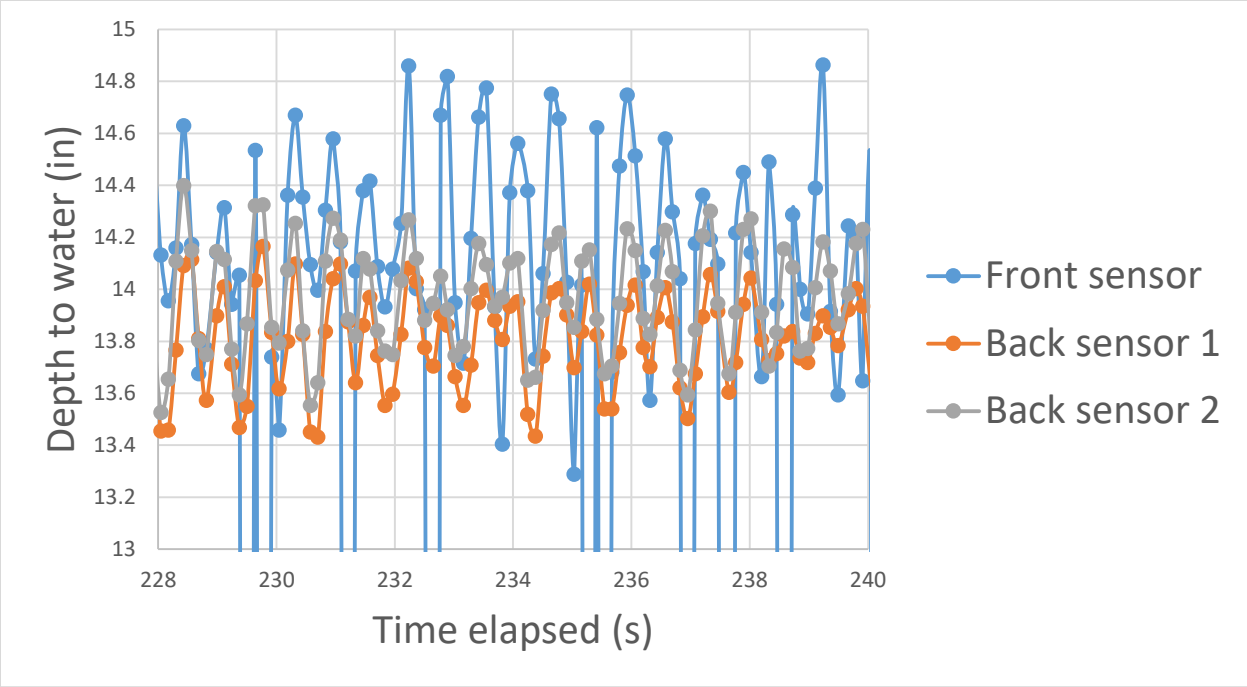

Figure 12: Example of wave measurement data with too many 0 values on a smaller scale

Figure 12 illustrates how the 0 values were often located at or near troughs in the wave form. The curvature of the water surface combined with the turbulence and the bubbles may have made it difficult for the sensor to accurately estimate the depth to water. Figure 12 also does not include any 0 values from the back sensors. As mentioned before, the waves were smoother on the back of the FWB model because of the wave attenuation.

The first attempt to resolve this issue was to make smoother waves on the front end. This proved difficult because the waves were generated by lifting water with a piece of wood. Although the wood did not completely come out of the water, it still created turbulence and bubbles in the water. The water lifted by the wood would propagate out in a circle from where the wood would come up. As a result, the sides of the wave generated would hit the side of the flume and bounce back towards the center of the flume. This resulted in an uneven wave form on the front end of

the FWB model. Since the wave generation was manually operated, these effects were mitigated as much as possible but were present to some extent in all runs.

The data from the ultrasonic sensors was validated using GoPro videos. Multiple runs for each frame configuration were filmed with a GoPro. Measuring sticks or tape were placed in front of and behind the FWB model and the movement of the water surface was captured by the GoPro. During data analysis, the peak and trough heights and times were recorded in an Excel sheet. From the peak and trough heights, wave heights were calculated and compared to the data from the ultrasonic sensors. The average wave heights from the GoPro video analysis are higher than the ones from the ultrasonic sensors. This can be explained by the fact that the GoPro filmed the side of the flume. The waves proceeded outward in an arc from the position where the piece of wood was lifted out of the water. As a result, the sides of a wave would move forward and towards the walls of the flume. When the side of a wave would hit the wall of the flume, the water would rise on the wall of the flume in the same way water rises at the end of a bathtub with moving water. This phenomenon causes the GoPro video data to be an overestimation of the wave heights in the run, hence explaining why these wave heights are higher than the ones measured by the ultrasonic sensors.

4.3.2 Pressure transducers

Another wave measurement method tested was the Solinst level logger model 3001 (Solinst, Georgetown, ON, Canada). This level logger is a pressure transducer that measure hydrostatic pressure multiple times per second. The data from the level logger is in mPa and can be converted to water level using the hydrostatic pressure equation:

$$P = \rho g h \tag{4}$$

Where P is the hydrostatic pressure in Pa,

ρ is the density of water in kg/m^3,

g is the gravitational constant in m/s^2, and

h is the water level above the pressure transducer.

The pressure transducer was placed at the bottom of the flume and collected hydrostatic pressure data during experimental runs. Figure 13 shows an example of water level data obtained from the level logger measurements.

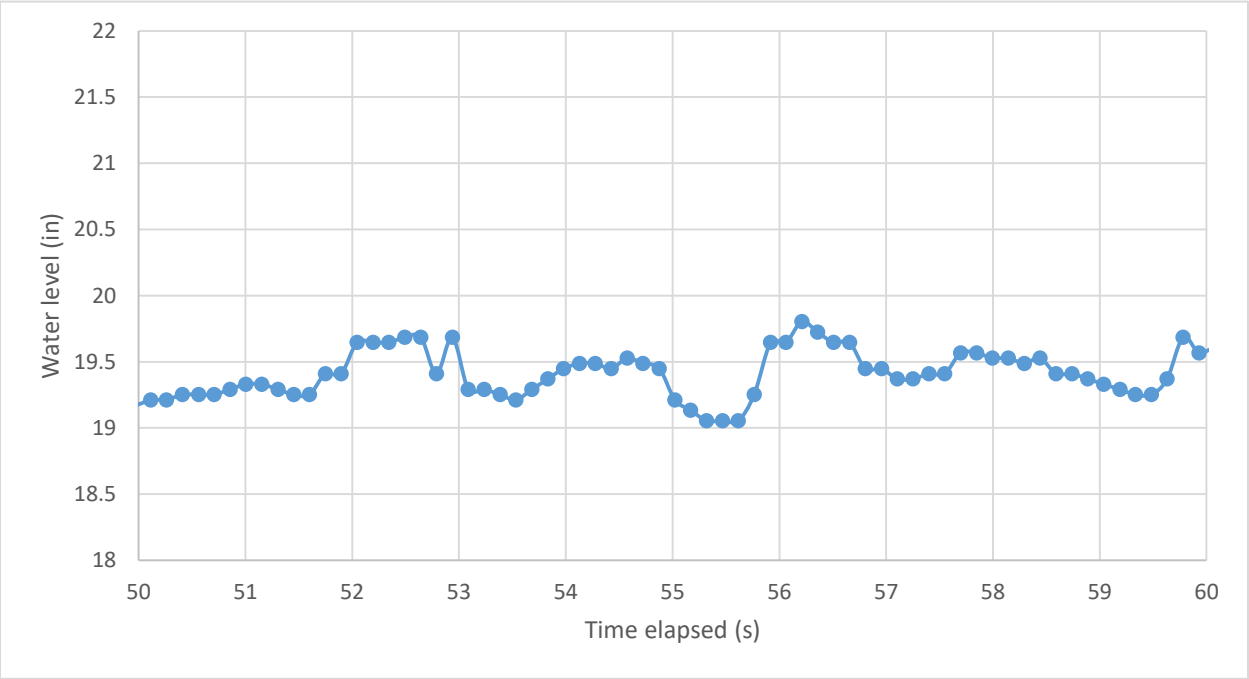

Figure 13: Example of water level data obtained from Solinst Model 3001 level logger

The data from the level logger did not accurately represent the wave profile observed during experimental runs and otherwise had smaller wave heights than the ones observed. For example, the wave profile in Figure 13 is estimated to show 5 waves in the over a period of 10 s which would result in a period around 2 s. This is outside of the 0.46 s to 0.81 s range of wave periods

that was maintained during the experimental runs. One reason why the pressure transducer data did not accurately represent the wave profile of the runs is that the water movement can affect the pressure measurements. It is possible that the force associated with the water movement of water in the flume affected the measurements of the pressure transducer. As a result, the pressure transducer would measure not only the hydrostatic pressure of the water above it, but also the pressure associated with the wave action in the flume.

4.3.3 eTape Fluid Level Sensor

Another wave measurement method used the eTape Continuous Fluid Level Sensor made by Milone Technologies (Milone Technologies, Sewell, NJ). The eTape measures electrical resistance which is affected by hydrostatic pressure to estimate water level. For this experiment, the eTape was glued to a piece of plexiglass and placed in the water. This apparatus is shown in Figure 14. The eTape was connected to an Arduino and with proper calibration, the water level on the tape could be estimated multiple times per second. This method was used in conjunction with the ultrasonic sensors in order to test it.

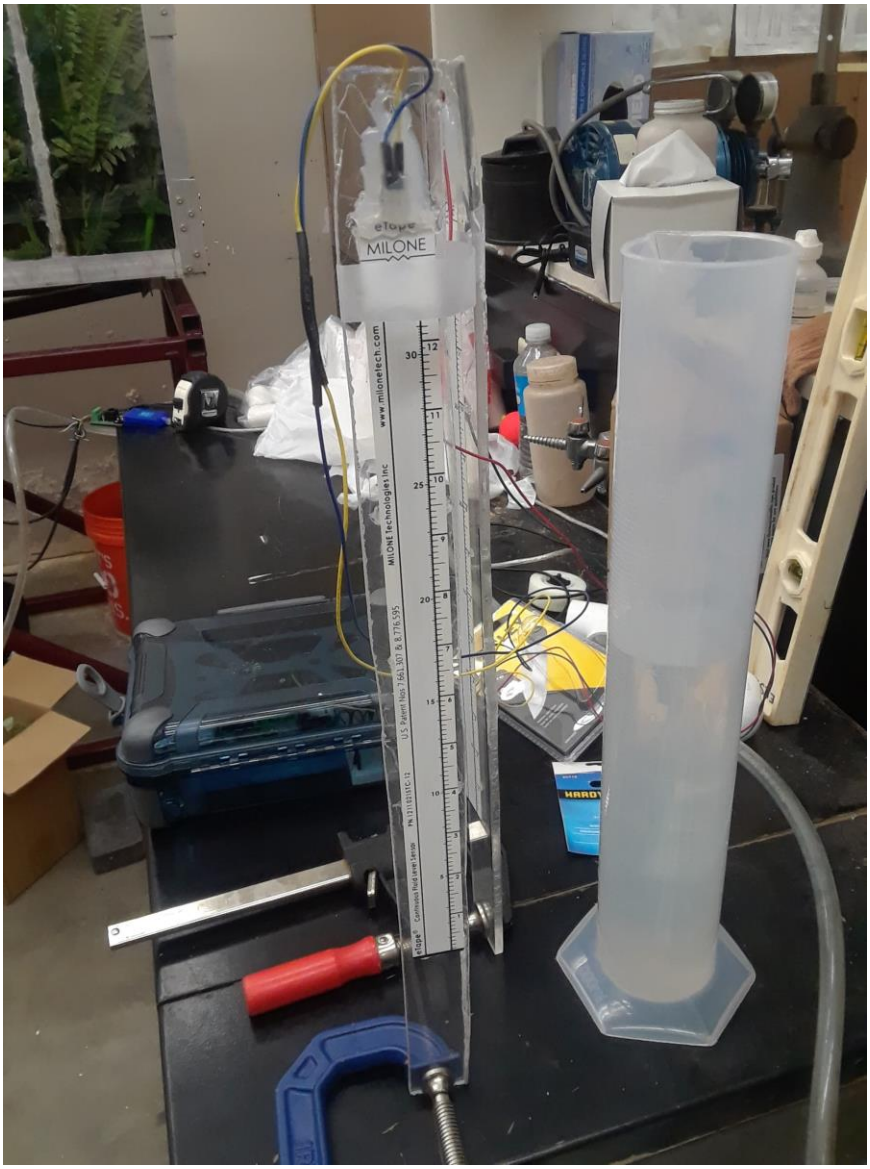

Figure 14: Picture of eTape (Milone Technologies, Sewell, NJ) sensor glued to a piece of plexiglass used in wave measurement experiments

A comparison of the data from the two methods on multiple runs determined that the wave heights measured by the eTape were consistently smaller than the ones measured by the ultrasonic sensors. Applying a correction factor to the data from the resistor tape was considered although determining such a factor would have required lots of data comparisons and yielded

less than accurate results. Figures 15 shows examples of data from an ultrasonic sensor and the eTape sensor over the same time frame of the same run. The wave profile from the ultrasonic sensor has taller waves than the wave profile from the eTape sensor.

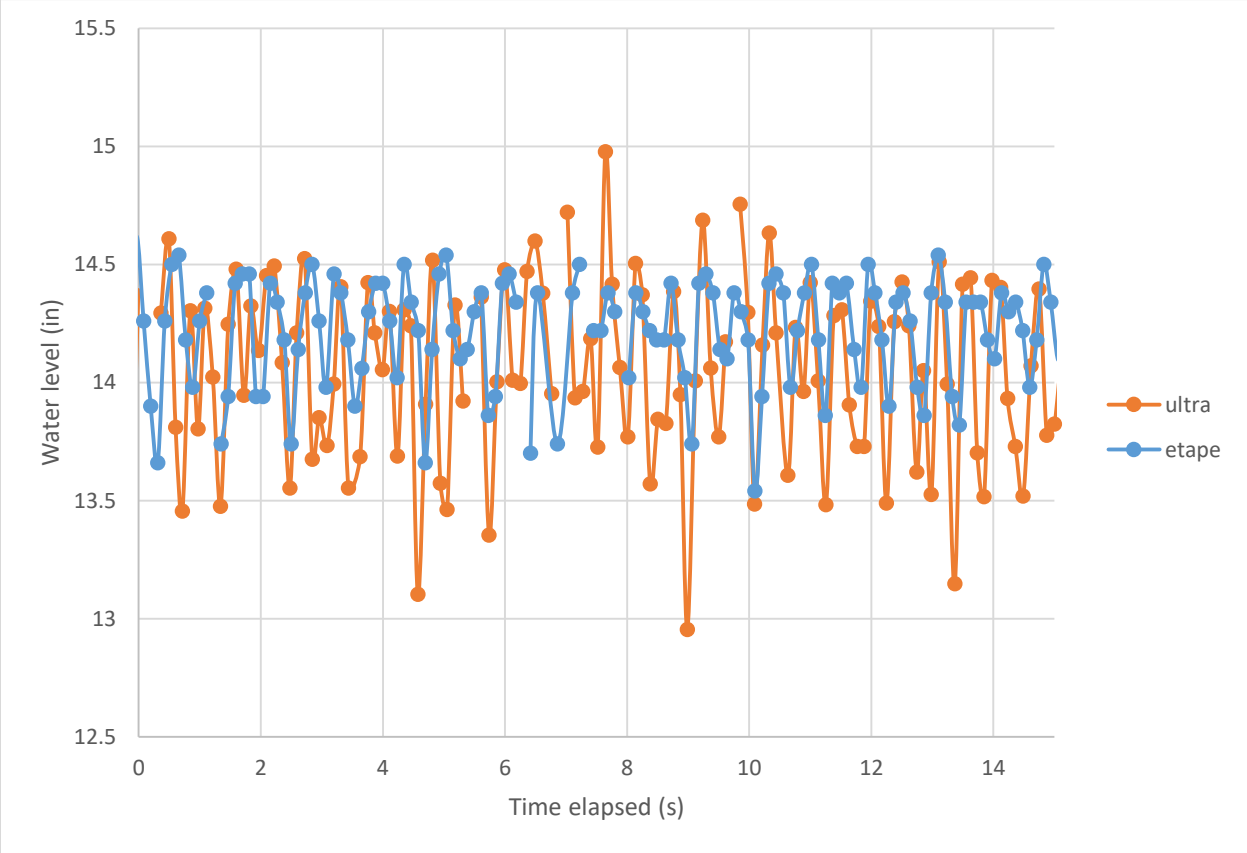

Figure 15: Example of data from ultrasonic sensor without 0 values compared to eTape (Milone Technologies, Sewell, NJ) data in the same time frame of the same run

4.3.4 Ultrasonic sensor with styrofoam ball

Another method used a floating Styrofoam ball with a flat piece of cardboard taped on top of it placed in a wire mesh cylinder under the ultrasonic sensor. As the ball would rise and fall with the water level and the sensor would be able to read the depth to the ball easier than the surface of the water. The ultrasonic sensor data had many 0 values, which prevented the analysis of such

data to yield accurate results. The wire mesh also had the potential to alter the wave form which would create a discrepancy between the measured wave heights and the wave heights that reached the FWB model. Figures 16 and 17 are pictures of the wire mesh cylinder and the Styrofoam ball used in this experiment. It is likely that the mesh cylinder and the Styrofoam ball did not reflect the ultrasonic signal from the sensor well. The ultrasonic sensor works best when used to measure the distance to a smooth surface. The wire mesh and the small Styrofoam ball most likely prevented the sensor from receiving its signal.

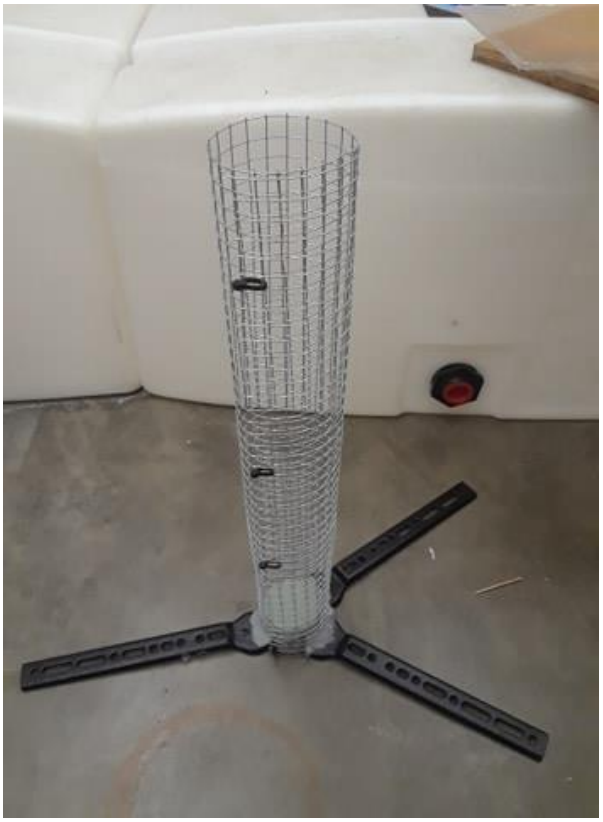

Figure 16: Wire mesh cylinder used in ultrasonic sensor with Styrofoam ball experiment

Figure 17: Styrofoam ball with flat piece of cardboard used in ultrasonic sensor with Styrofoam ball experiment

4.3.5 Ultrasonic sensor with plastic sheet

Ultimately, the most effective method consisted in laying a thin sheet of plastic wrap on the water surface under the sensor. The sheet of plastic was attached at the top of the flume so it would not be displaced by the waves. Runs were stopped if bubbles accumulated under the plastic sheet in order to avoid errors in measurement from the sensors. The sheet of plastic smoothed the wave enough for the sensor to read it adequately. The waves that reached the FWB model were the same waves that were measured by the sensor even though they were smoothed out by the plastic film. This method worked well for this experiment's purposes and allowed for the completion of the data collection.

4.4 Data Analysis

After data collection, the videos were manually analyzed using the VLC Media Player (VideoLAN, Paris, France) video software. Oklahoma Water Survey employees uploaded the

videos from the runs and recorded the peak height, peak time, trough height and trough time for each wave in Microsoft Excel. Wave height, or amplitude, was calculated as the difference between a peak height and the adjacent trough height. Wave period was calculated as the time between two consecutive peaks. Average wave heights and wave periods, as well as the average of the highest third of the wave heights for each run were calculated. From the data, the energy density of the waves was calculated using the following equation from Holthuijsen (2007):

$$E = \frac{1}{16}\rho g H_{m0}^2 \quad (5)$$

where:

E is the energy density of waves in J/m^2

ρ is the density of water in kg/m^3

g is the acceleration due to gravity in m/s^2

H_{m0} is the significant wave height calculated as the average of the highest third of the wave heights measured

This equation is empirical and may not be effective in conditions that differ from the original study. Also, this equation may not yield representative results for runs that have an uneven distributions of wave heights (Holthuijsen, 2007). Because only the top third of the waves are considered, a run that has mostly large waves and small waves can have a higher wave energy density value than a run that has an even distribution of wave heights, even though they may have the same average wave height. Wave height and energy results were compared between the two scales tested. For each FWB frame configuration, wave height results were compared between the prototype scale and the normalized 1:8 scale. In order to compare both data sets, the

1:8 scale wave height results were multiplied by the length scale factor of 8. The 1:8 scale wave-energy density were multiplied by 64 since the length term is squared in the wave-energy density equation used (Equation 4). The normalized standard error of measurement was calculated by dividing the standard error by the average wave height or wave energy density of a particular FWB configuration at a specific scale. Standard error values were calculated using the Microsoft Excel "steyx" function.

The Mann-Whitney U test was used to determine if there was a significant difference between the wave-height and wave-energy density distributions from both scales. The method for the Mann-Whitney U test described by Laerd Statistics was performed using the IBM SPSS 26 software (IBM, Armonk, NY). The Mann-Whitney U test is a non-parametric statistical test used to compare differences between two independent groups when the dependent variable is either ordinal or continuous, but not normally distributed (Laerd Statistics). The Mann-Whitney U test is used to test whether two samples are likely derived from the same population by comparing the medians of those samples. The Mann-Whitney U test has four main assumptions. The first assumption is that the dependent variable is at the ordinal or continuous level. In this study, the dependent variable is either wave height or wave-energy density which are continuous variables. The second assumption is that the independent variable consists of two or more groups. Here, the independent variable is wave height or wave-energy density and the data is divided in groups based on scale or frame configuration. The third and fourth assumptions are that the observations are independent and that the two distributions being compared have the same shape. Observations are independent because they each represent a different experimental run. However, due to lack of data, the fourth assumption could not be verified, but is assumed. A confidence level of 95% was used for the Mann-Whitney U test.

Chapter 5 - Results and Discussion

Wave reduction experiments by FWBs at two different scales have been completed. Wave-height and energy-density results are compared between FWB skirt wall configurations and between scales, followed by the statistical analysis of the data using the Mann-Whitney U test. In addition, wave periods are discussed. Finally, the different wave measurement methods used in the experiments and discussed to elucidate lessons learned from trying various methods at the small scale. The compiled wave measurement results (Tables A1-A3), the Python code used to collect data from the ultrasonic sensors (Table A4) and the wave measurement results used for statistics calculations in IBM SPSS (Table A5) are located in the attachments on ShareOK.

5.1 Results and Comparison of Wave Height and Energy Reduction for Various Floating-Wetland Breakwater Skirt Wall Configurations at Two Scales

Wave heights and energy densities on the front and back of the FWBs were first investigated for each scale. Figures 18 and 19 show the wave height and energy results for the prototype scale, and figures 20 and 21 show the wave height and energy results for the 1:8 scale. Wave height and energy data are grouped by pipe length and number of pipes in the skirt wall.

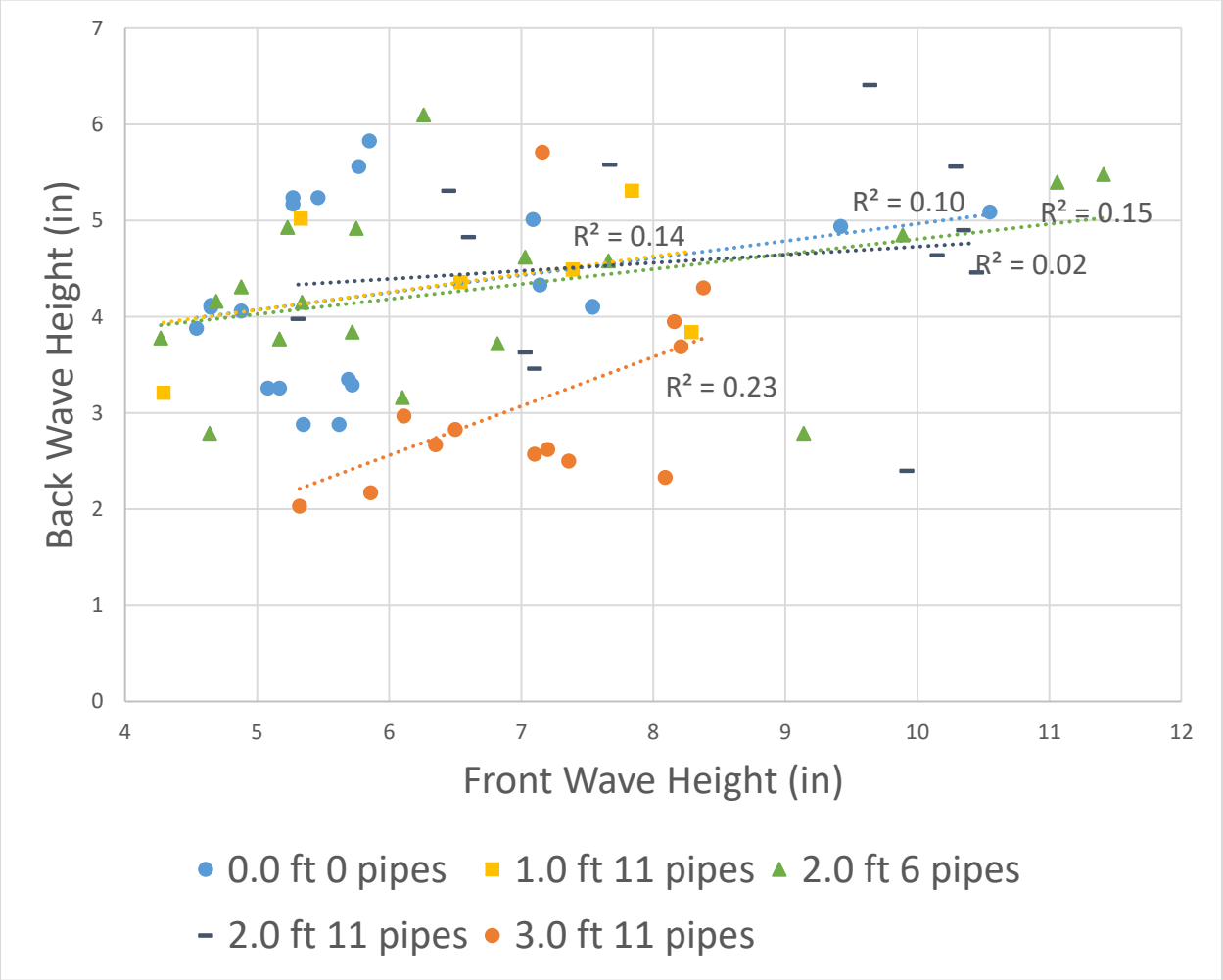

Figure 18: Wave heights on the front and back of the FWBs for prototype system. "X.0 ft Y pipes" refers to the length and number of pipes hanging down as the skirt wall of the FWB.

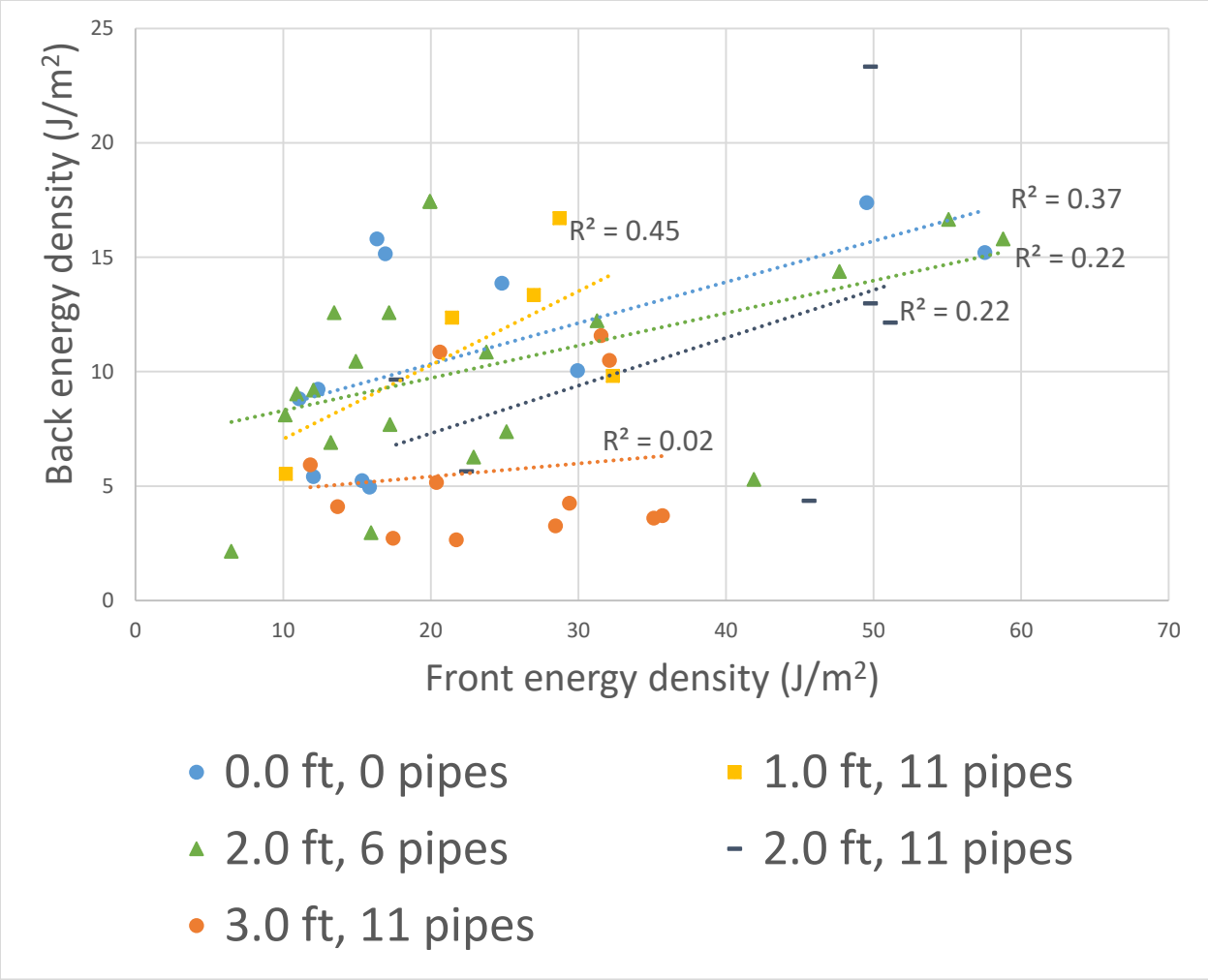

Figure 19: Wave energy densities on the front and back of the FWBs for prototype system. "X.0 ft, Y pipes" refers to the length and number of pipes hanging down as the skirt wall of the FWB.

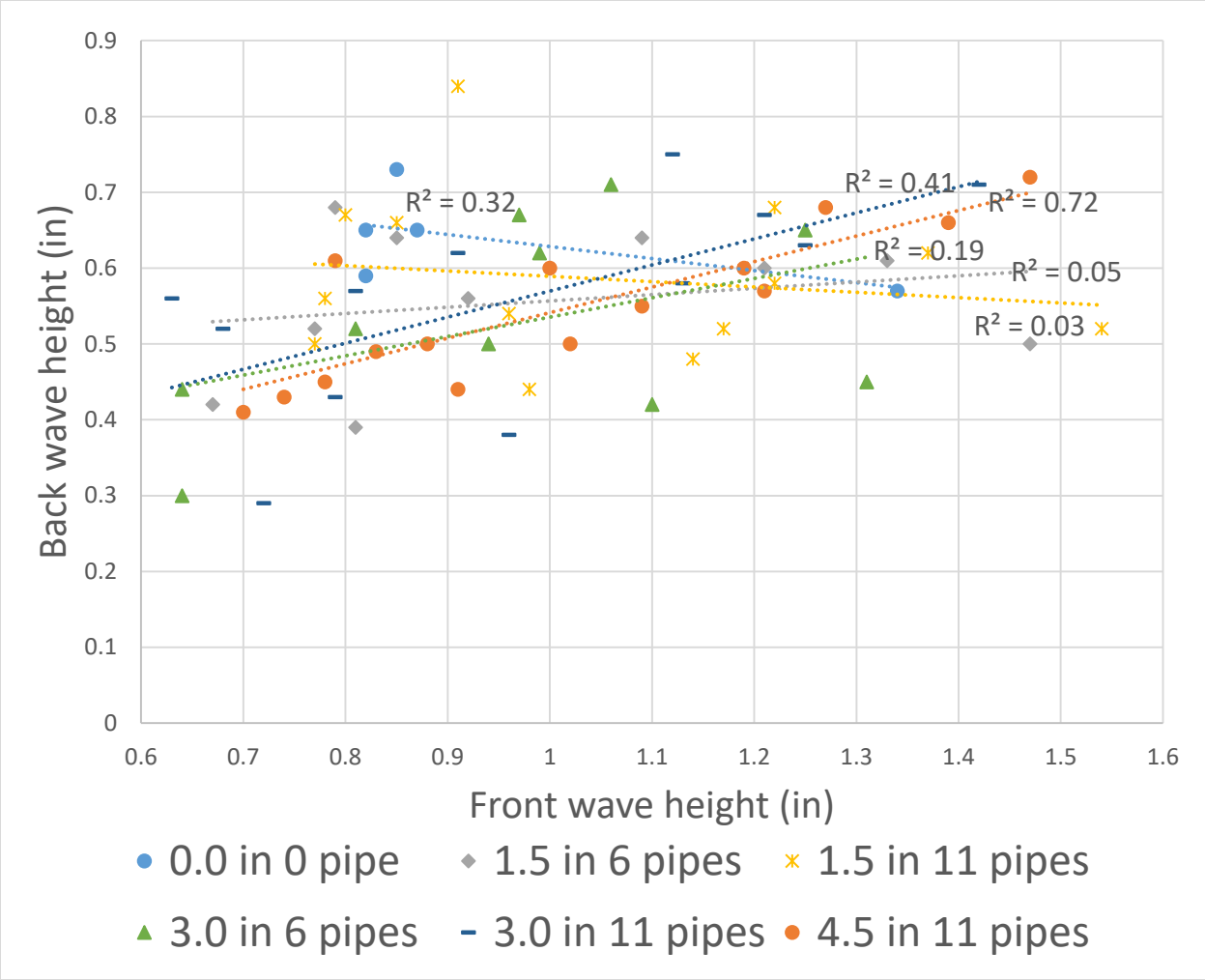

Figure 20: Wave heights on the front and back of the FWBs for 1:8 scale system. "X.0 in Y pipes" refers to the length and number of pipes hanging down as the skirt wall of the FWB.

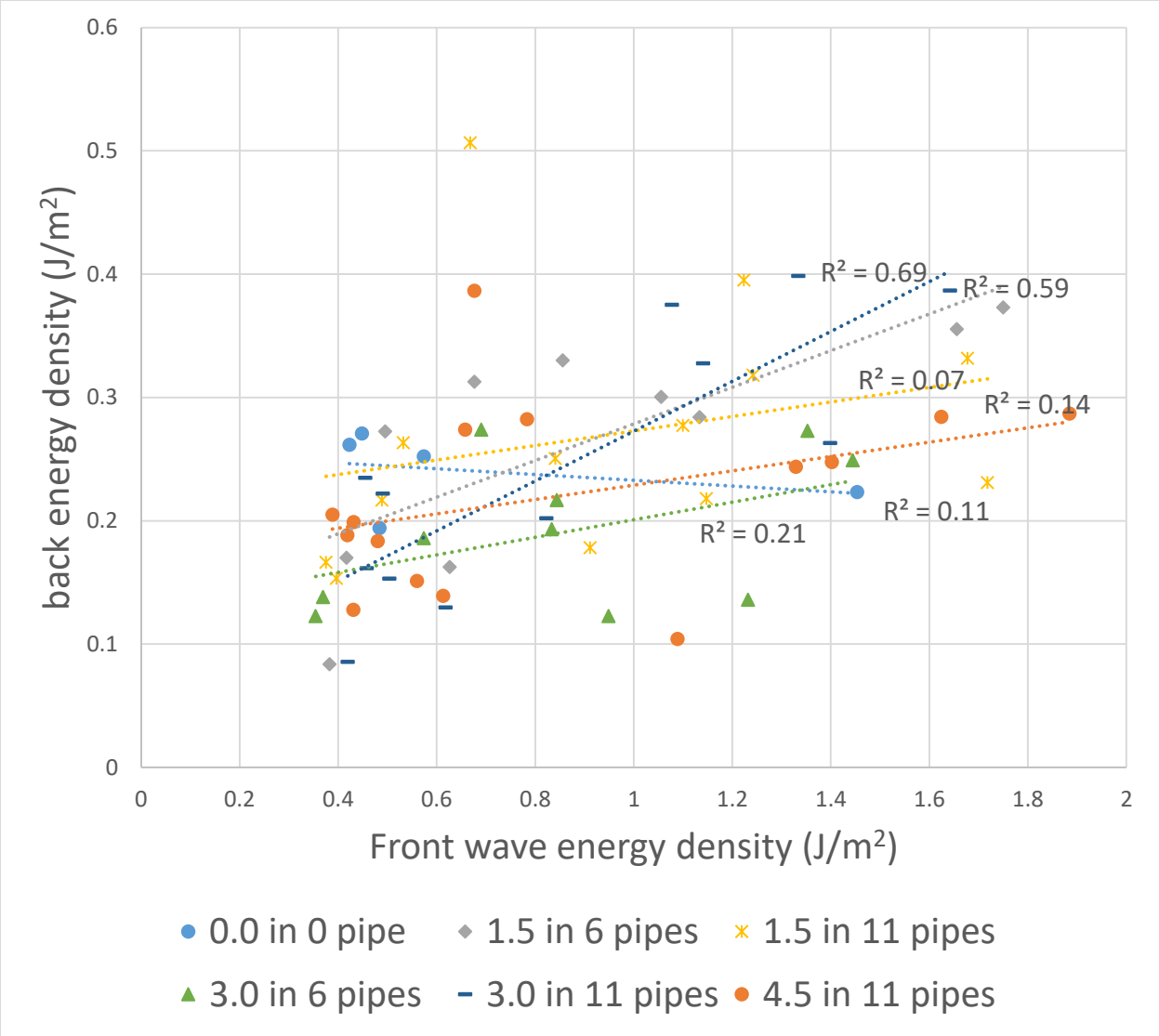

Figure 21: Wave energy densities on the front and back of the FWBs for 1:8 scale system. "X.0 in Y pipes" refers to the length and number of pipes hanging down as the skirt wall of the FWB.

The wave height and wave-energy density data exhibit a high degree of variability. Out of the 26 trendlines from the four graphs presented in figures 18-21, only 4 have R^2 coefficients greater than 0.50. This may be due to the inherent variability of waves as well as the error included in the measurement methods such as video analysis. A visual comparison between skirt wall configurations for the prototype scale (figures 18 and 19) would suggest that the 3.0 ft, 11 pipes

frame had the best wave reduction performance. The trendlines for that frame are placed lower than the others, though the R^2 values associated with the trendlines are 0.23 in figure 18 and 0.02 in figure 19. Visually, the data does not suggest that increasing skirt wall pipe length and number of pipes increases the wave reduction performance of FWBs. These observations will be further investigated in the statistical analysis section.

5.2 Comparison Between Scales

The wave reduction performance of each FWB frame configuration was compared between the two scales. Figures 22 – 26 show the wave-height results on the front and back of the FWBs. Figures 27 – 31 show the same comparison but based on wave-energy density. Here, the results are normalized for scale. This means that for the 1:8 scale, wave-height values were multiplied by 8 and wave-energy density values were multiplied by 64. For the 1:4 scale, wave-height values were multiplied by 4 and wave-energy density values were multiplied by 16. Data for the 1:4 scale was limited to the 0.0 in 0 pipe configuration because of a lack of experiments explained in Chapter 6.

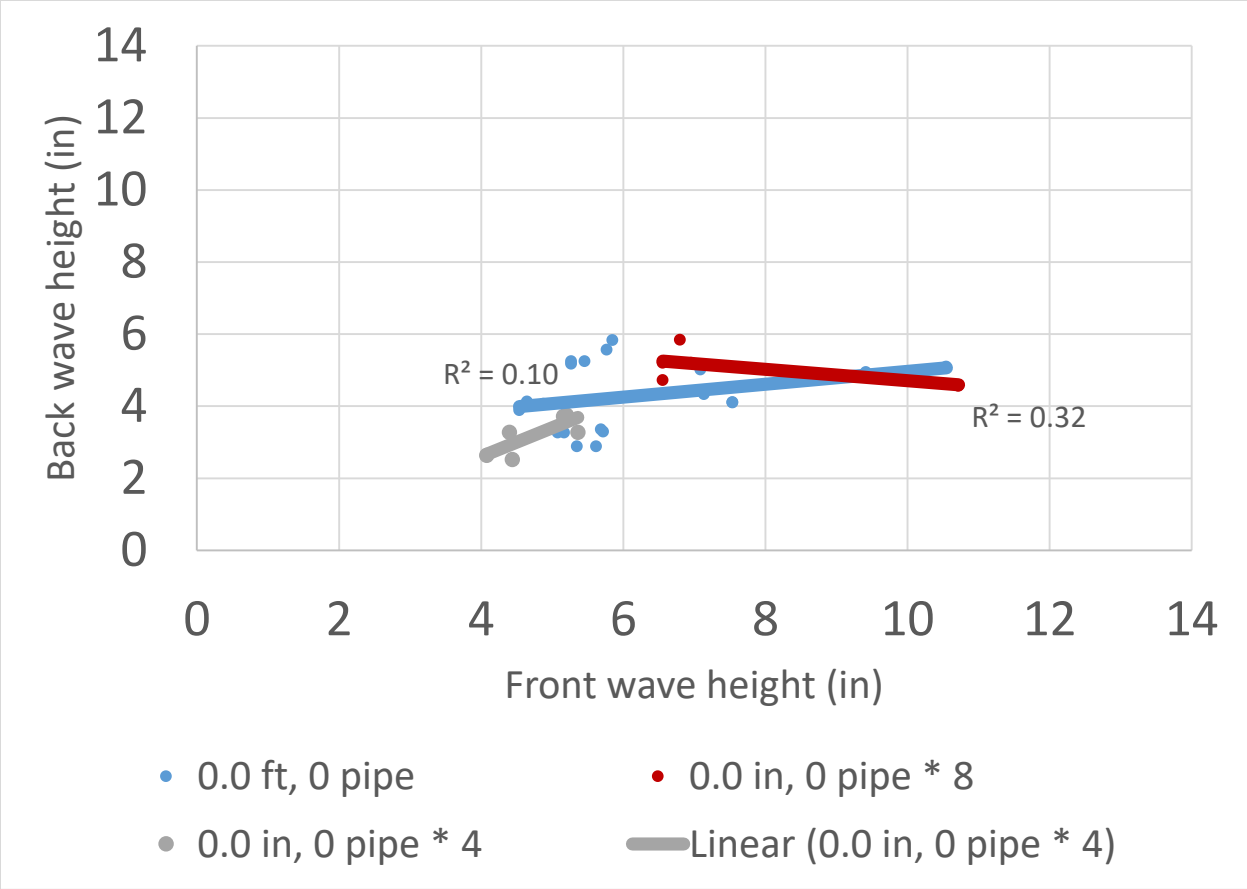

Figure 22: Wave height results scale comparison for 0.0 ft 0 pipe. "X.0 ft, Y pipes" refers to the length and number of pipes hanging down as the skirt wall of the FWB, and * refers to the scale multiplier.

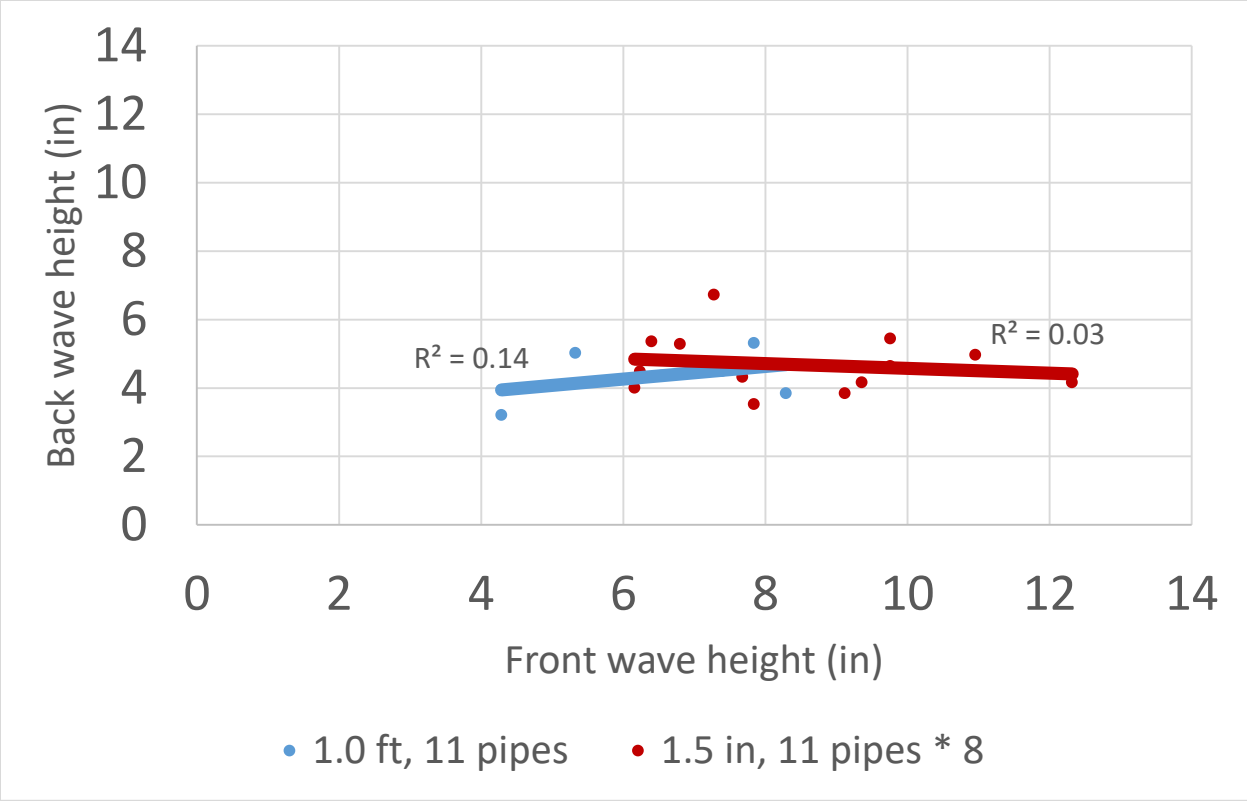

Figure 23: Wave height results scale comparison for 1.0 ft 11 pipes. “X.0 ft Y pipes” refers to the length and number of pipes hanging down as the skirt wall of the FWB, and * refers to the scale multiplier.

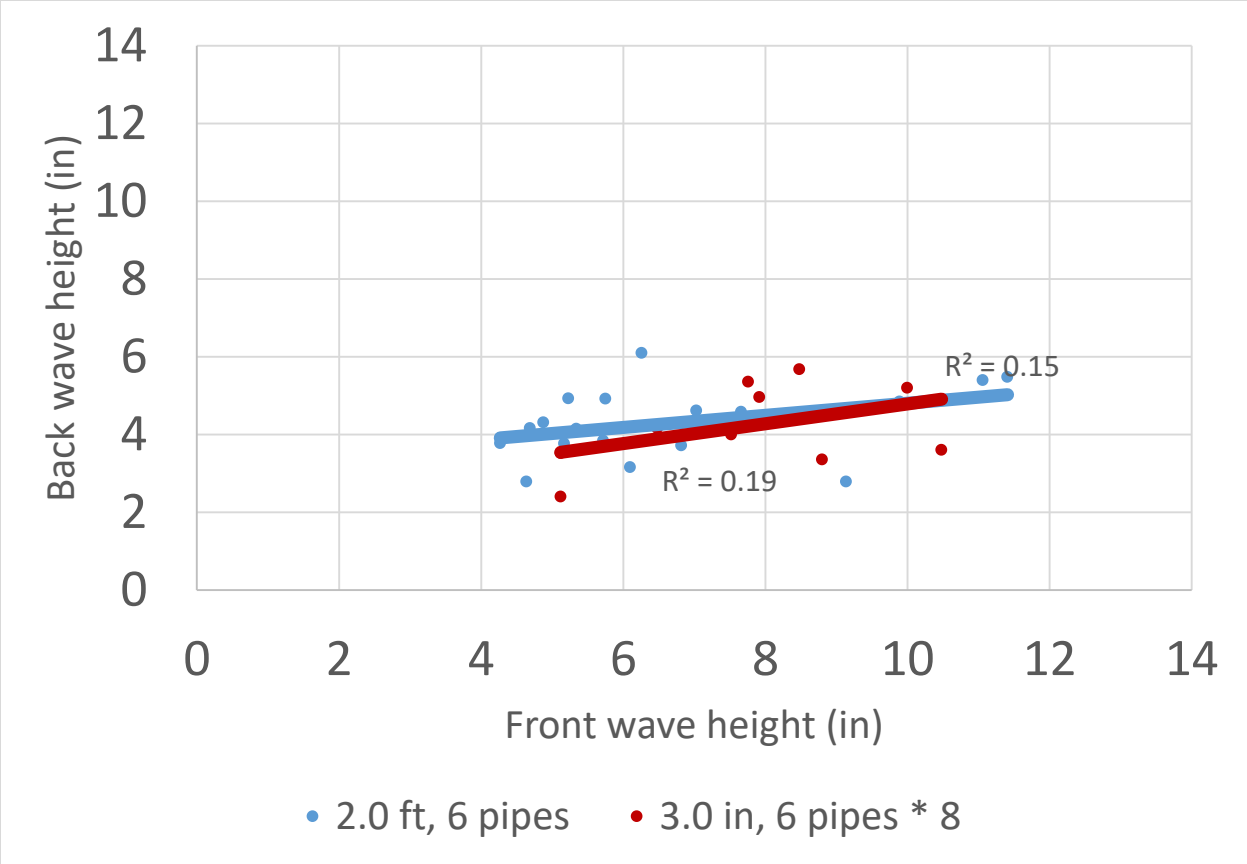

Figure 24: Wave height results scale comparison for 2.0 ft 6 pipes. “X.0 ft Y pipes” refers to the length and number of pipes hanging down as the skirt wall of the FWB, and * refers to the scale multiplier.

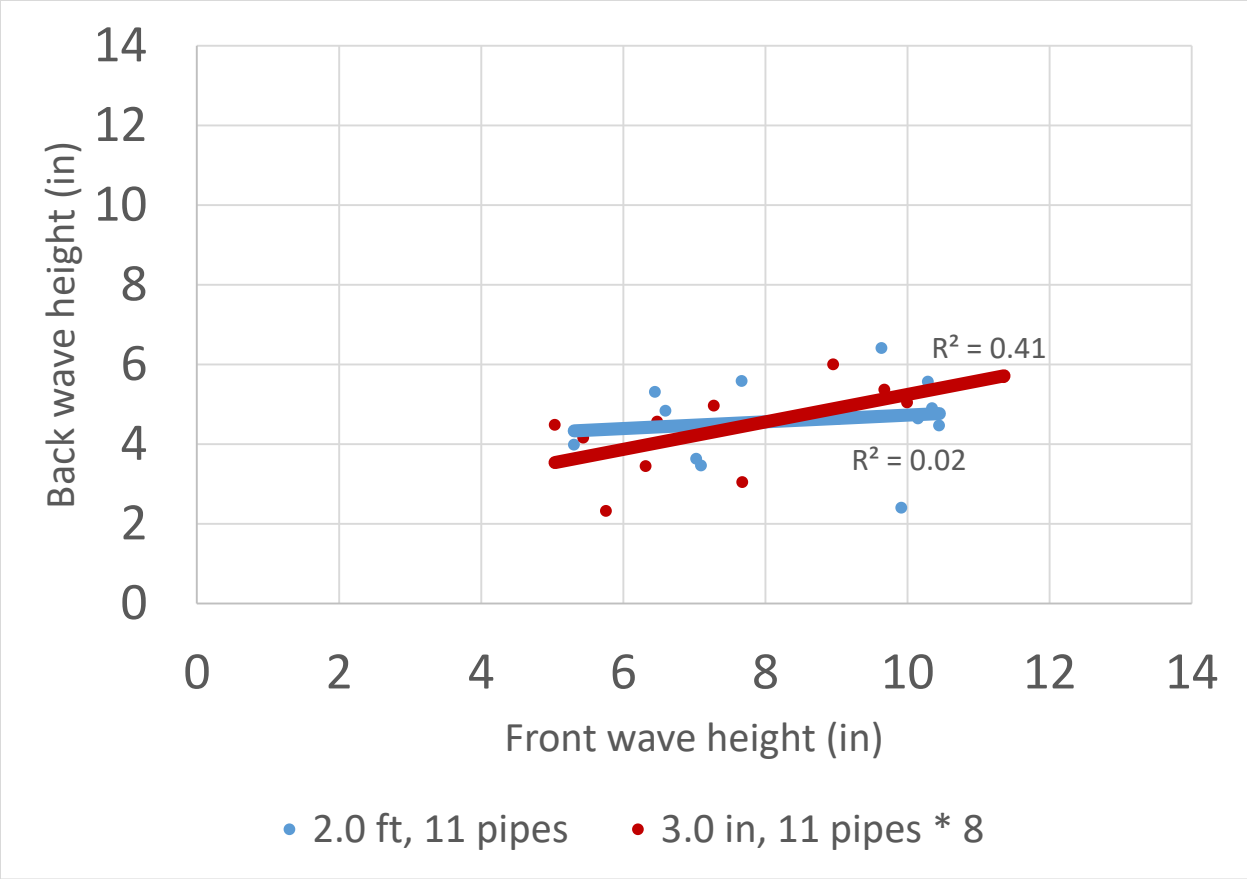

Figure 25: Wave height results scale comparison for 2.0 ft 11 pipes. “X.0 ft Y pipes” refers to the length and number of pipes hanging down as the skirt wall of the FWB, and * refers to the scale multiplier.

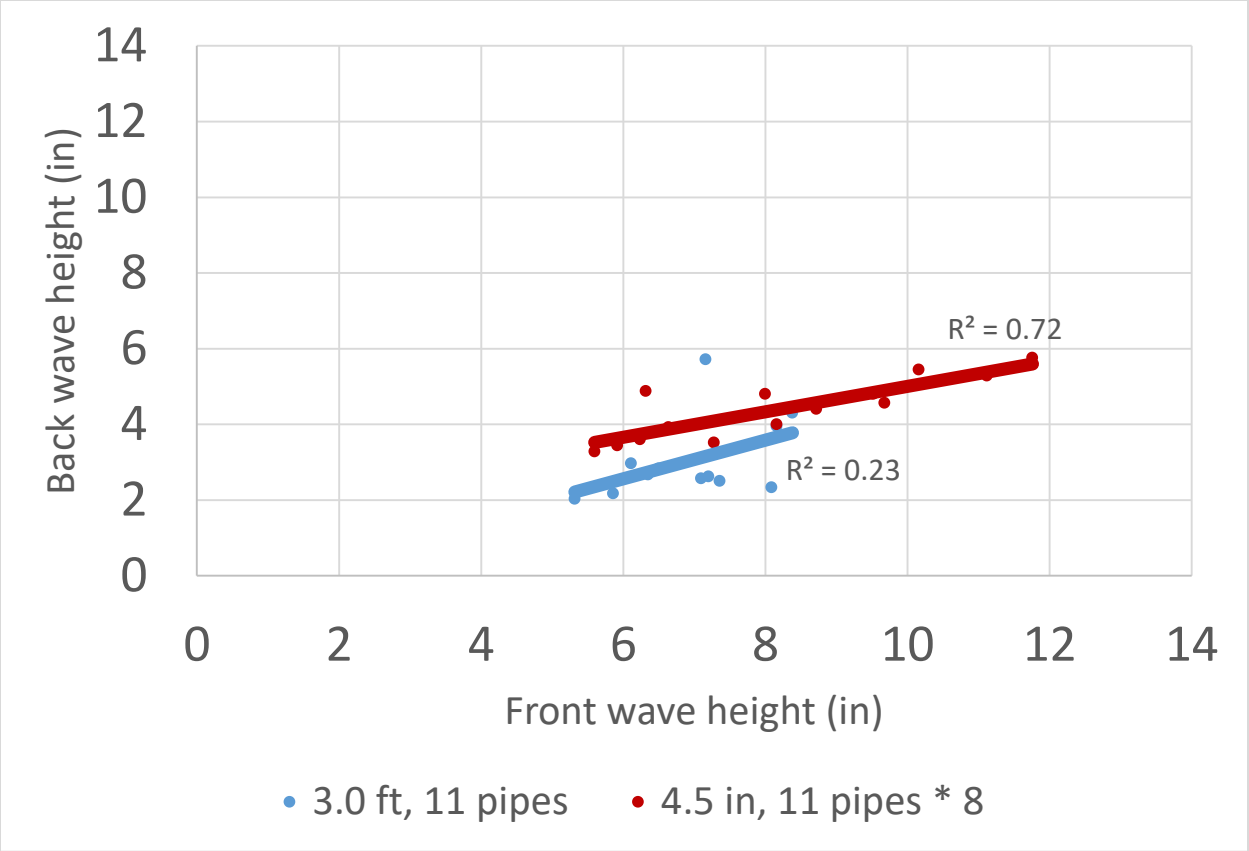

Figure 26: Wave height results scale comparison for 3.0 ft 11 pipes. “X.0 ft Y pipes” refers to the length and number of pipes hanging down as the skirt wall of the FWB, and * refers to the scale multiplier.

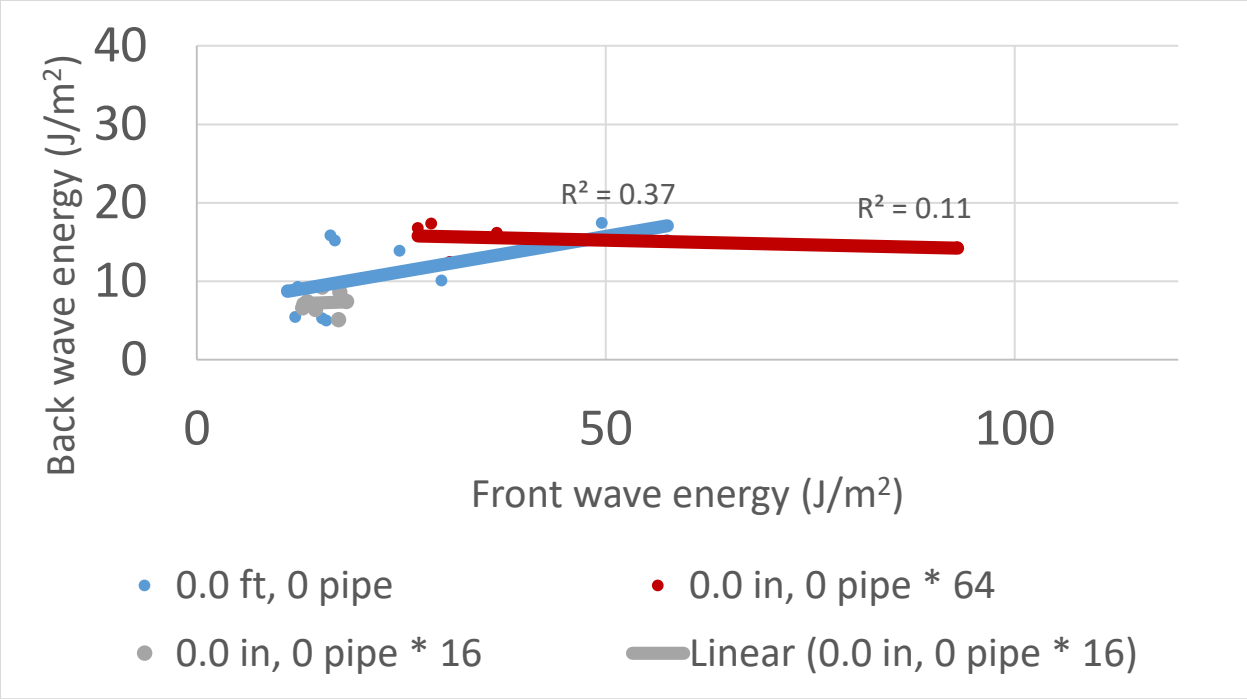

Figure 27: Wave-energy density results scale comparison for 0.0 ft 0 pipe. “X.0 ft Y pipes” refers to the length and number of pipes hanging down as the skirt wall of the FWB, and * refers to the scale multiplier.

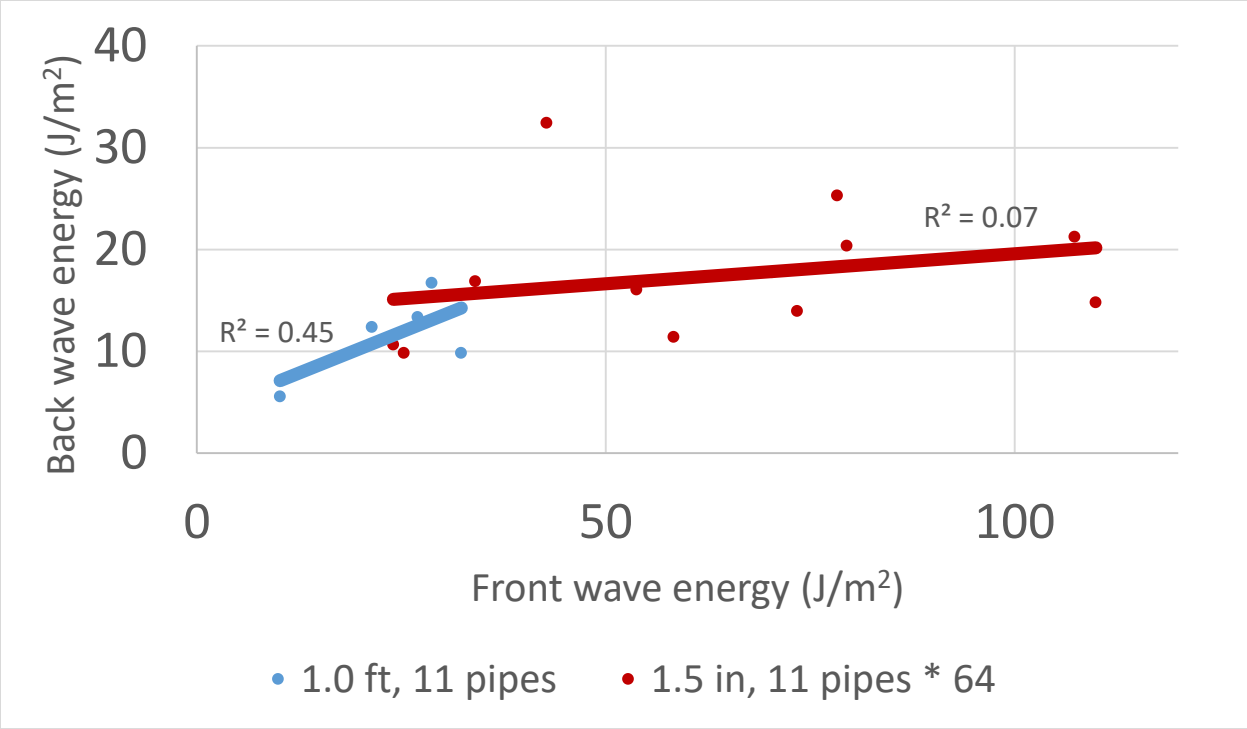

Figure 28: Wave-energy density results scale comparison for 1.0 ft 11 pipes. “X.0 ft Y pipes” refers to the length and number of pipes hanging down as the skirt wall of the FWB, and * refers to the scale multiplier.

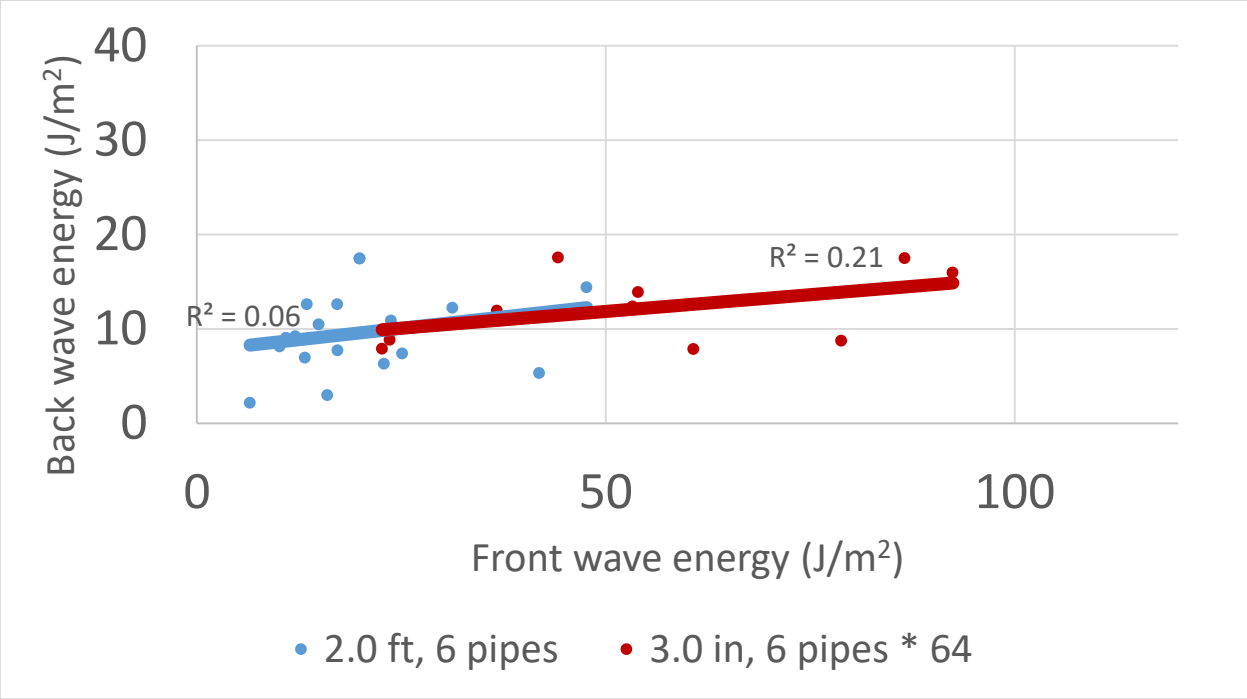

Figure 29: Wave-energy density results scale comparison for 2.0 ft 6 pipes. “X.0 ft Y pipes” refers to the length and number of pipes hanging down as the skirt wall of the FWB, and * refers to the scale multiplier.

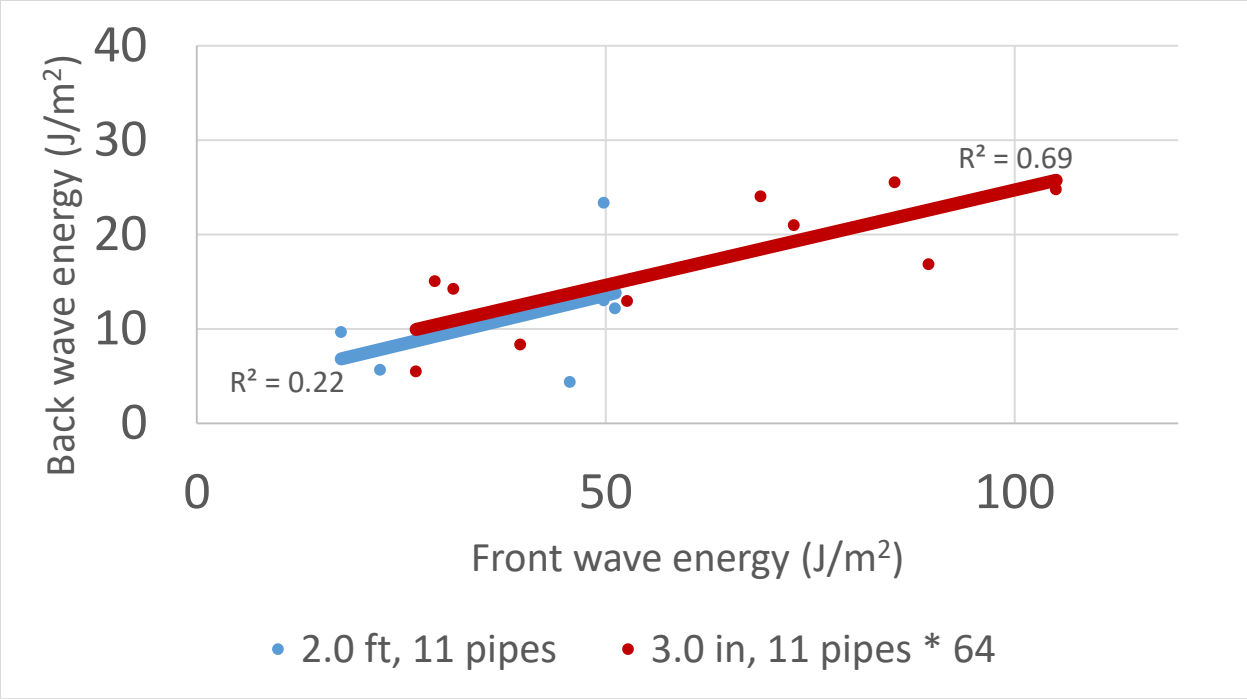

Figure 30: Wave energy density results scale comparison for 2.0 ft 11 pipes. "X.0 ft Y pipes" refers to the length and number of pipes hanging down as the skirt wall of the FWB, and * refers to the scale multiplier.

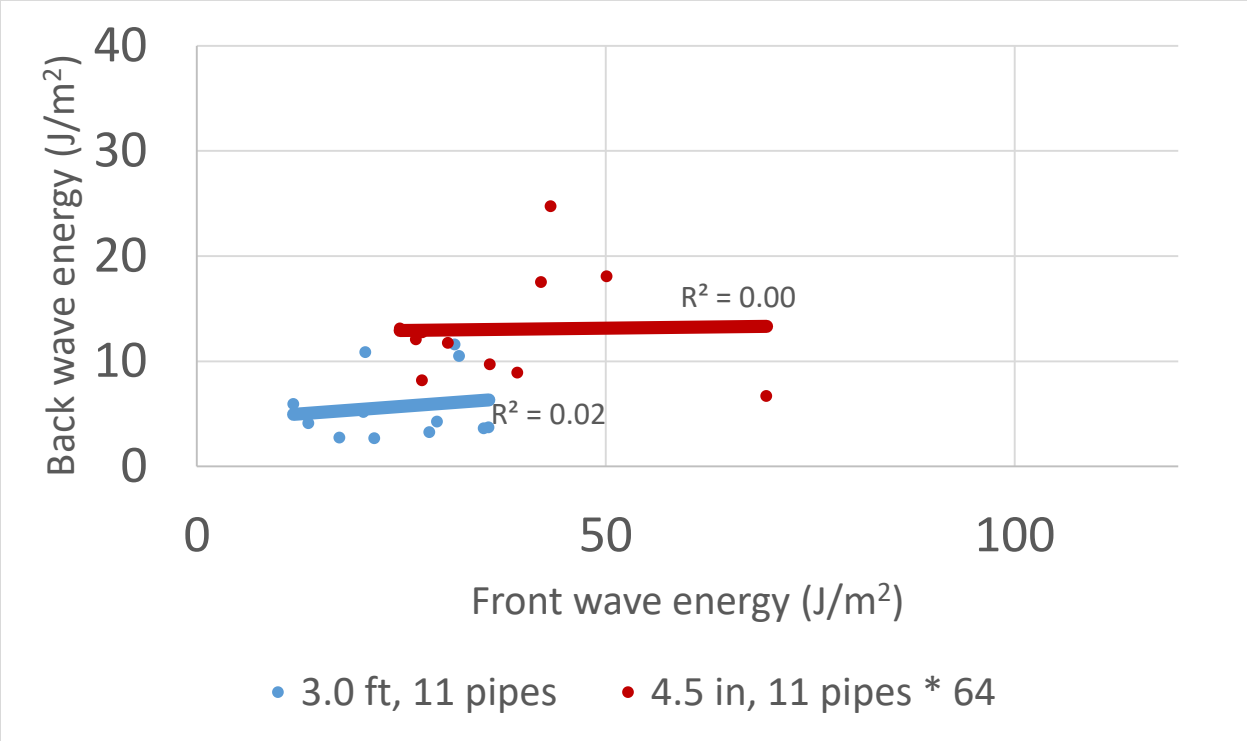

Figure 31: Wave energy density results scale comparison for 3.0 ft 11 pipes. "X.0 ft Y pipes" refers to the length and number of pipes hanging down as the skirt wall of the FWB, and * refers to the scale multiplier.

For the scale comparison, the data has a high degree of variability with 16 out of the 24 trendlines in Figures 22-31 having an R^2 value less than 0.20. Visually, most of the trendlines for the wave height and the wave-energy density graphs overlap. This would suggest that the wave reduction performance of FWBs at different scales is comparable. This is not the case for the 3.0 ft 11 pipes frame where the trendlines are distinct from each other on the wave height as well as the wave-energy density graphs (figures 27 and 31). This frame is the exception in this data set and suggests that the prototype scale performed better than the 1:8 scale as the trendline for the

prototype data is placed lower that of the 1:8 scale data. These observations are further investigated in the statistical analysis section.

5.3 Statistical Analysis

The Mann-Whitney U test was used to compare the wave height and wave-energy density between the prototype scale and the model scale for the different FWB skirt wall configurations that were tested (Table 1). This statistical analysis is used to compare the wave reduction performance between the two scales. The Mann-Whitney U test found no significant difference in wave height reduction between the prototype scale and the 1:8 scale FWB frames except for the 0.0 ft 0 pipe frame and the 3.0 ft 11 pipes frames. The Mann-Whitney U test found no significant difference in wave-energy density reduction between the prototype scale and the 1:8 scale FWB frames except for the 2.0 ft 6 pipes and the 3.0 ft 11 pipes frames. As mentioned in the visual analysis, the 3.0 ft 11 pipes distribution showed better wave reduction than the other frame configurations at the prototype scale whereas at the 1:8 model scale it performed similarly to the other frames. This difference became more apparent in the scale comparison figures 26 and 31 where the two distributions were distinct from each other. This difference is confirmed by the Mann-Whitney U test indicating a significant difference between the two scales for this frame configuration. The Mann-Whitney U test found no significant difference in wave reduction for six out of the 10 frames tested and the only frame configuration where both the wave height and the wave-energy density distributions were significantly different was the 3.0 ft 11 pipes frame. This suggests that the FWBs at the prototype scale and at the model scale performed similarly. The 3.0 ft 11 pipes frame seems to be an exception in this investigation and the reason for this will be explored later in section 5.5. For the 2.0 ft 6 pipes frame, the wave reduction performance was significantly different when comparing wave energy density but not

when comparing wave height. As mentioned in Section 4.4, the wave energy density equation used in this study is empirical and may yield results that are not representative for certain runs. Figure 29 shows the comparison of wave energy density results between the two scales. The model scale results have a different range of values than the prototype scale results. This could have affected the results of the Mann-Whitney U test and yielded a low p value.

Table 1: p values (95% CI) for Mann-Whitney U test comparing prototype scale and 1:8 model scale wave height and wave-energy density distributions for different FWB skirt wall configurations.

	Skirt wall configuration	**p value**
Wave height	0.0 ft 0 pipe	0.01
	1.0 ft 11 pipes	0.64
	2.0 ft 6 pipes	0.51
	2.0 ft 11 pipes	0.65
	3.0 ft 11 pipes	<0.01
Wave-energy density	0.0 ft 0 pipe	0.09
	1.0 ft 11 pipes	0.06
	2.0 ft 6 pipes	0.04
	2.0 ft 11 pipes	0.18
	3.0 ft 11 pipes	<0.01

To investigate the effect of skirt-wall pipe length and number of pipes on FWB wave reduction, the Mann-Whitney U test was used to compare the wave height and energy density results from

the different FWB configurations tested to one another. Tables 2-5 show the p values for the Mann-Whitney U test comparing these FWB configurations.

Table 2: p values (95% CI) from Mann-Whitney U test comparing wave height results of different FWB skirt wall configurations at the model scale. p values less than 0.05 are highlighted.

FWB skirt wall configuration	**0.0 in 0 pipe**	**1.5 in 6 pipes**	**1.5 in 11 pipes**	**3.0 in 6 pipes**	**3.0 in 11 pipes**	**4.5 in 11 pipes**
0.0 in 0 pipe		0.129	0.246	0.165	0.234	0.098
1.5 in 6 pipes			0.693	0.796	0.872	0.765
1.5 in 11 pipes				0.313	0.979	0.387
3.0 in 6 pipes					0.628	0.849
3.0 in 11 pipes						0.648

Table 3: p values (95% CI) from Mann-Whitney U test comparing wave energy density results of different FWB skirt wall configurations at the model scale. p values less than 0.05 are highlighted.

FWB skirt wall configuration	**0.0 in 0 pipe**	**1.5 in 6 pipes**	**1.5 in 11 pipes**	**3.0 in 6 pipes**	**3.0 in 11 pipes**	**4.5 in 11 pipes**
0.0 in 0 pipe		0.254	0.849	0.165	0.879	0.612
1.5 in 6 pipes			0.784	0.052	0.674	0.177
1.5 in 11 pipes				0.042	0.538	0.217
3.0 in 6 pipes					0.254	0.311
3.0 in 11 pipes						0.614

Table 4: p values (95% CI) from Mann-Whitney U test comparing wave height results of different FWB skirt wall configurations at the prototype scale. p values less than 0.05 are highlighted.

FWB skirt wall configuration	**0.0 ft 0 pipe**	**1.0 ft 11 pipes**	**2.0 ft 6 pipes**	**2.0 ft 11 pipes**	**3.0 ft 11 pipes**
0.0 ft 0 pipe		0.798	0.945	0.365	0.001
1.0 ft 11 pipes			0.721	0.553	0.012
2.0 ft 6 pipes				0.439	0.001
2.0 ft 11 pipes					0.005

Table 5: p values (95% CI) from Mann-Whitney U test comparing wave energy density results of different FWB skirt wall configurations at the prototype scale. p values less than 0.05 are highlighted.

FWB skirt wall configuration	**0.0 ft 0 pipe**	**1.0 ft 11 pipes**	**2.0 ft 6 pipes**	**2.0 ft 11 pipes**	**3.0 ft 11 pipes**
0.0 ft 0 pipe		0.827	0.792	0.884	0.006
1.0 ft 11 pipes			0.575	0.662	0.014
2.0 ft 6 pipes				0.929	0.006
2.0 ft 11 pipes					0.024

The results from Tables 2-5 indicate that there is generally no significant difference in wave height and energy density reduction between the different FWB configurations tested. However, the 3.0 ft 11 pipes configuration results are significantly different from those of all other configurations at the prototype scale when considering both wave height and wave energy density. These results confirm the visual inspection of the distributions where the 3.0 ft 11 pipes distribution was distinct from the other distributions at the prototype scale but not at the 1:8 scale. At the model scale, the 1.5 in 11 pipes configuration and the 3.0 in 6 pipes configuration are also significantly different when comparing wave energy density results. The 3.0 in 6 pipes configurations seems to perform better than the 1.5 in 11 pipes configuration.

5.4 Wave-period Analysis

Wave-period results were investigated to determine if they had an effect of the wave-height and wave-energy density reduction by FWBs. Figure 32 shows the wave-height reduction percentage as a function of the wave period at the 1:8 scale. Figure 33 shows the wave period values behind the FWBs in relation to the wave period values in the front at the 1:8 scale.

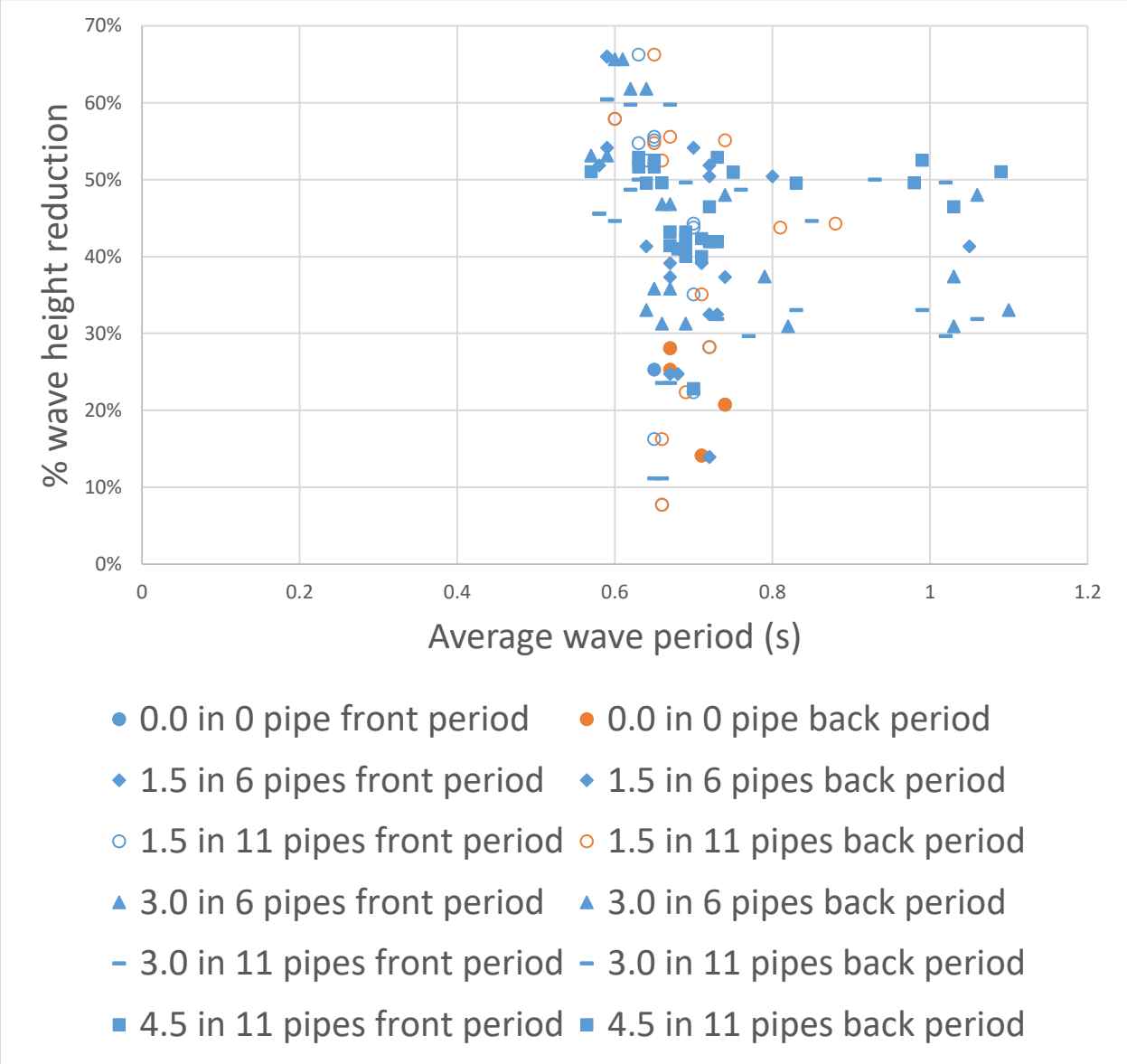

Figure 32: Percent wave height reduction as a function of average wave period at the 1:8 scale

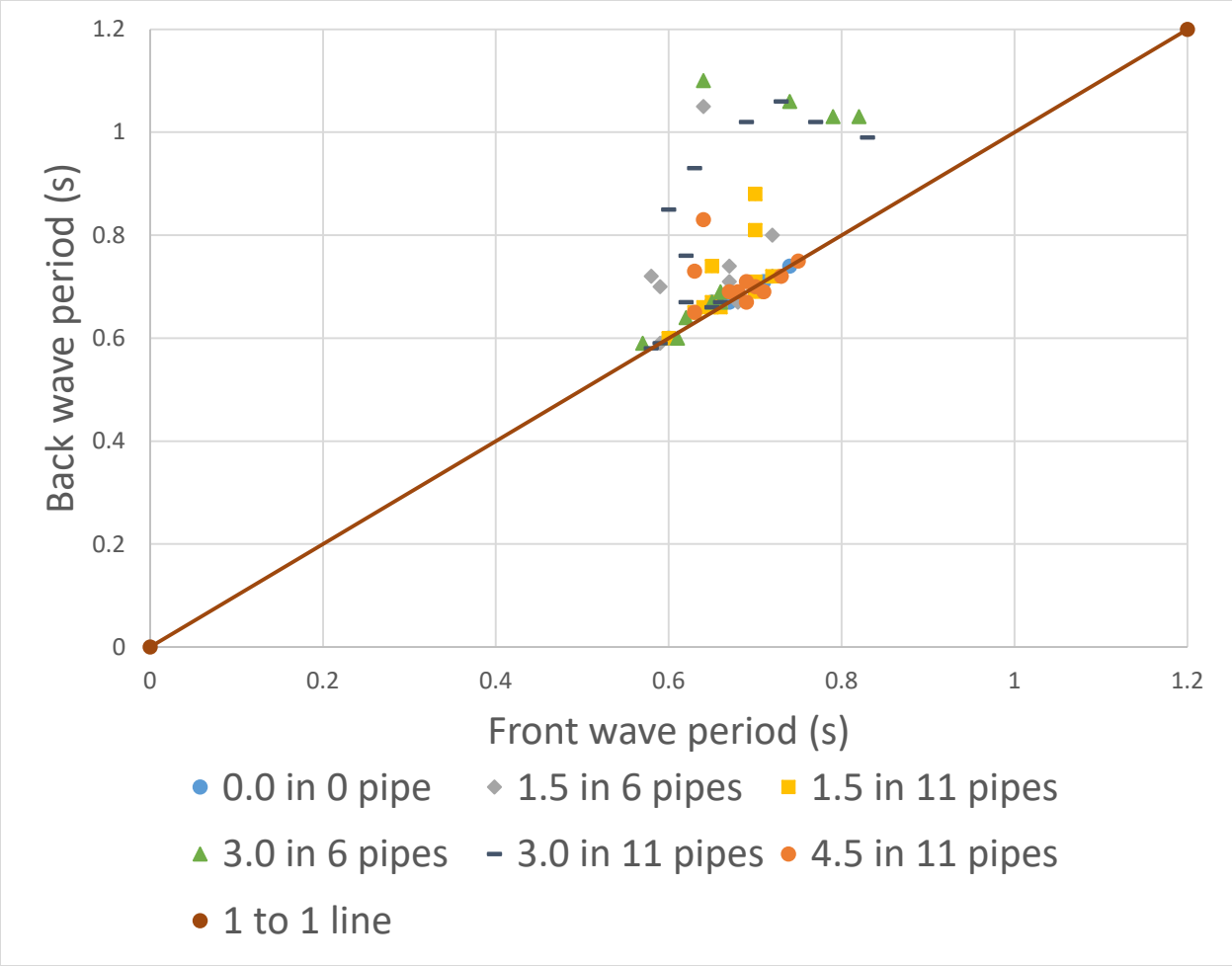

Figure 33: Wave period values behind the FWBs vs in the front at the 1:8 scale. X in Y pipes refers to the length and number of pipes hanging down as the skirt wall of the FWB

Figure 32 shows that the wave periods in the front of the FWBs are in the desired range of 0.46 s and 0.81 s as determined by the scaling method. Within this range of wave period values, percent wave height reduction values range from 6% to 66%.

Wave period values are often near the 1:1 line when comparing in front of and in back of the FWB (Figure 33). However, wave period values are occasionally higher in the back than in the front. The ultrasonic sensors measured depth to water every 0.12 seconds on average. This time

interval is used to determine whether points are on or off the 1:1 line. Any point where the back wave period is more than 0.12 seconds greater than the front wave period is considered to be off the 1:1 line. The difference in wave period between the front and back of the FWBs can be due to the turbulence that is often present in front of the FWBs. The wave generation at the 1:8 scale caused turbulence and created a busy wave profile and a relatively small wave period. As waves hit the FWBs, only the main wave profile remained and many of the smaller waves were completely dampened. As a result, fewer, smoother waves were found behind the FWBs and this caused the wave period to be a bit higher. Runs where the average back wave period was higher than the average front wave period usually had higher average wave heights. This investigation indicated that wave periods did not affect wave height and energy density reduction within the range tested.

5.5 Normalized Measurement Standard Error Analysis

The wave height and energy density data from experimental runs visually has a high degree of variability. The investigation of the error of measurement associated with these data can help explain the results of the statistical analysis. The standard error of the wave height and energy density results was calculated using the “steyx” function of Excel. This standard error was then normalized by dividing by the mean of the distribution. This calculation was performed for each skirt wall configuration at the prototype scale and the model scale. Table 6 is a compilation of the normalized standard error values calculated.

Table 6: Normalized standard error values for wave height and wave-energy density results for each FWB skirt wall configuration at the prototype scale and the 1:8 scale

	1:8 Model Scale		Prototype scale	
	Wave height	Wave-energy density	Wave height	Wave-energy density
0.0 ft 0 pipe	0.09	0.14	0.21	0.35
1.0 ft 11 pipes	0.18	0.24	0.18	0.31
2.0 ft 6 pipes	0.19	0.37	0.20	0.40
2.0 ft 11 pipes	0.24	0.30	0.25	0.59
3.0 ft 11 pipes	0.20	0.25	0.31	0.61

The normalized standard-error values for wave-height and wave-energy density at the prototype scale are similar or higher than those at the 1:8 scale. For the 0.0 ft 0 pipe and the 3.0 ft 11 pipes configurations, the normalized standard error values are 1.5 to almost 3 times higher at the prototype scale than at the 1:8 scale. These configurations were also determined to have significantly different distributions by the Mann-Whitney U test. This would suggest that the FWBs have a statistically similar wave height and energy reduction performance at the prototype scale and the 1:8 scale although this is not true of the 0.0 ft 0 pipe and the 3.0 ft 11 pipes configurations. This discrepancy may be due to the high standard error associated with the results from these configurations. The model scale results have normalized standard error values that are less than those of the prototype scale results, which can be due to the model system being more easily controlled than the prototype system. The model system was located in a flume inside a temperature-regulated laboratory. The prototype system on the other hand, was

located outside in a pond where it could be affected by wind and weather. These conditions could have led to greater variability in the results.

5.6 Wave-reduction Comparison

The wave-height reduction results from this study were compared to those of other studies on floating breakwaters. Wave height reduction is often calculated using the wave transmission coefficient, K_t. The wave transmission coefficient is calculated is the transmitted wave height or back height divided by the incident or front height. The ranges of wave transmission coefficients found in the studies of Neelamani (2018), Uzaki (2011) and Ozeren (2009) were compared to those found in this study at the prototype scale and at the 1:8 scale as shown in Table 7.

Table 7: Range of wave transmission coefficient values for floating breakwaters on other studies and FWBs in this study.

	Kt range			
	Literature	Prototype scale	Model scale	Description
Neelamani (2018)	0.58 - 0.84			Pontoon floating breakwater with varying skirt wall sizes
Uzaki (2011)	0.3 - 1.0			2.0 m wide floating breakwater with 0.6 m water depth
Ozeren (2009)	0.2 - 0.9			Cylindrical floating breakwater
0.0 ft 0 pipe		0.49-0.99	0.72-0.86	
1.0 ft 11 pipes		0.47-0.95	0.34-0.92	
2.0 ft 6 pipes		0.31-0.98	0.34-0.69	
2.0 ft 11 pipes		0.43-0.83	0.40-0.89	
3.0 ft 11 pipes		0.29-0.80	0.47-0.77	

The ranges of wave transmission coefficients found in this study are similar to those found in other studies. The maximum wave transmission coefficient are also similar across studies, except for the study by Neelamani. This suggests that the FWBs used in this study exhibit similar performance as non-wetland floating breakwaters from these studies.

5.7 Further Discussion of the 3.0 ft 11 pipes FWB Configuration

The 3.0 ft 11 pipes FWB configuration results have differed from those of other FWB skirt wall configurations in this study. At the prototype scale, the 3.0 ft 11 pipes configuration visually seemed to perform better than other configurations. The wave height and energy density results of this configuration were significantly different than those of the other configurations which suggests that the 3.0 ft 11 pipes frame performed better statistically. At the 1:8 scale, the corresponding FWB configuration visually and statistically performed similarly to other configurations, and was significantly different than the 3.0 ft 11 pipes configuration at the prototype scale. The wave period investigation determined that the runs where the wave period was smaller on the front side than on the backside of the FWB were the runs with the highest average wave heights. The 3.0 in 6 pipes configuration had multiple runs where the front wave period was greater than the back wave period. This could explain why the wave energy density results of this configuration were significantly different from the 1.5 in 11 pipes configuration. The 3.0 ft 11 pipes distribution results at the prototype scale had the highest normalized standard error values. This high degree of variability could explain why the 3.0 ft 11 pipes distributions were significantly different between the prototype scale and the 1:8 scale. The wave height and energy density reduction results of the 3.0 ft 11 pipes were both significantly different between the prototype scale and the 1:8 scale. More investigation is required to determine if pipe length and number of pipes in the skirt wall affect the wave reduction performance of FWBs. Table 8 summarizes relevant results from the wave reduction study. According to the linear trendlines generated, the 3.0 ft 11 pipes configuration provides the best wave height reduction at an 8-in incident wave at the prototype scale whereas the 1.0 ft 11 pipes configurations has the best reduction for a 1-in wave at the model scale. The 3.0 ft 11 pipes configuration did not have many

runs where the back wave period was much higher than the front wave period. One possible reason why the 3.0 ft 11 pipes configuration performed better than other configurations at the prototype scale is the weight of the FWB. At the prototype scale, the FWBs were made of relatively thicker PVC pipe than at the model scale. Also, the PVC pipes in the skirt wall were connected with metal braces that were much denser than PVC. Since the 3.0 ft 11 pipes had the longest pipes and the highest number of pipes and metal braces in the skirt wall, it had the most additional weight of all the configurations tested. This could have affected the submergence and the resistance to movement of the FWB which improve wave reduction (Ozeren, 2009). At the model scale, the PVC pipes used were relatively thinner and the connections in the skirt wall were also made of PVC. As a result, the 4.5 in 11 pipes configuration which corresponds to the 3.0 ft 11 pipes configuration, did not have much additional weight compared to other configurations. This could explain why the 4.5 in 11 pipes configuration performed similarly to the other configurations and differently when compared to the 3.0 ft 11 pipes configuration. More insight on the 3.0 ft 11 pipes configuration may be provided in the upcoming thesis of Maxwell O'Brien (School of Civil Engineering & Environmental Science), which is investigating the implementation of this FWB configuration in a reservoir.

Table 8: Summary of relevant findings from wave reduction study

	Back wave height (in) for 8 in (prototype) and 1 in (model) incident wave				
	Prototype scale	Model scale	Percentage of runs not on the wave period 1:1 line (%)	Scale comparison p values(wave height)	Scale comparison p values (wave energy density)
0.0 ft 0 pipe	4.61	0.63	0	0.01	0.09
1.0 ft 11 pipes	4.63	0.39	8	0.64	0.06
2.0 ft 6 pipes	4.5	0.54	40	0.51	0.04
2.0 ft 11 pipes	4.56	0.57	50	0.65	0.18
3.0 ft 11 pipes	3.58	0.54	33	<0.01	<0.01

Chapter 6 - Conclusions, Lessons Learned and Future Work

The main goal of this study was to determine how scale affects the wave height and energy density reduction of FWBs. To achieve this, wave reduction experiments were conducted on FWBs at different scales and with different skirt wall configurations. Multiple wave measurement methods were attempted at the model scale. The final method used ultrasonic sensors and a sheet of plastic on the water surface to reduce turbulence. The comparison between scales determined that the wave height and energy density reduction of FWBs was similar at the

prototype scale and the 1:8 scale although the 3.0 ft 11 pipes configuration differed from the other frames. The comparison between FWB skirt wall configurations showed that the 3.0 ft 11 pipes configuration was significantly different from other configurations at the prototype scale although their equivalents at the 1:8 scale were not significantly different. This could be attributed to the additional weight of PVC pipe thickness and metal connectors on the 3.0 ft 11 pipes FWB. This additional weight could have affected the submergence and resistance to movement of the FWB and therefore its wave reduction performance. The analysis of normalized standard error determined that the 3.0 ft 11 pipes configuration had the highest standard error. The wave period investigation did not yield a relationship between wave period and wave height reduction. Also, experimental runs with high average wave heights were more likely to have a higher wave period on the backside of the FWB than on the front side. A comparison of wave transmission coefficients between this study and studies on floating breakwater in literature showed that the wave transmission coefficients calculated in this study are similar in range and maximum values to the ones found in other studies.

Retrospectively, a few aspects of this study could have been done differently to gain better insight into the wave reduction performance of FWBs. One such aspect of this study is the estimation of wavelength. Studies from Uzaki (2011) and Ozeren (2009) suggest that the depth to wavelength ratio affect the wave reduction performance of floating breakwaters. Wavelength could have been calculated by multiplying wave velocity and wave period. Wave velocity could have been measured using an anemometer during the experimental runs. Dynamic similitude between the prototype and the model was not fully achieved because the FWBs at the prototype scale had metal connectors in the skirt wall whereas the model scale FWBs had PVC connectors.

This resulted in a density discrepancy in the scaling and could have yielded better wave reduction results for the FWBs at the prototype scale.

This Master of Science thesis research study has been a learning experience for those involved. The first lesson learned in this project was that waves are difficult to control. Water waves are not only affected by the wave generation method but also by wind and air pressure, water depth, the shape and material of the tank or reservoir, etc. Because of this, generating waves of different heights and speeds can feel like an art more than a science. Determining the appropriate wave measurement method was an iterative process that made clear how important it is to be able to adapt to available technology. Finding an appropriate wave measurement method with time and financial constraints required creative thinking. Another learning experience was the data analysis process. The lack of available research on this research topic coupled with the lack of data acquired in this study made it challenging to derive defendable conclusions from the results obtained. Understanding the wave reduction performance of FWBs at different scales required an extensive data analysis process with theoretical, visual and statistical considerations.

This study has determined that FWBs generally have a similar wave reduction performance at the different scales tested. However, more work is required to better understand the wave reduction from FWBs. Experimenting on more scales would have helped determine the relationship between scale and wave reduction performance with more certainty. Plans were made to test a 1/4 scale but data collection was halted before completion due to the advent of the COVID-19 pandemic in the United States starting in March 2020. Collecting more data would help provide more certainty in the results obtained. Field experiments can also be supplemented with spectral analysis. Future work could also include investigating the role of the weight of the FWBs and their placement in the water column on their wave reduction performance. Lighter,

more buoyant FWBs sitting higher in the water column than heavier or more tightly anchored FWBs may exhibit different wave reduction performances. The anchoring method of the FWBs also affects wave height reduction according to Ozeren (2011). His study determined that a concrete pile anchoring system yielded better wave reduction results than a mooring system. The FWBs used in this study were moored to the bottom of the basin. Their performance could be improved by anchoring them using piles. Another addition to this research would be to add plants to mimic a FWB as it would be implemented and determine the result on wave reduction. In this study, the wave motion was perpendicular to the face of the FWBs. However, FWBs in reservoirs are subjected to waves from multiple directions. Investigating the attenuation of oblique waves could provide more insight into the performance of FWBs in reservoirs.

The FWBs in this study were only allowed to pitch and heave because of their position in the pond or flume and their anchoring pattern. Further studies could estimate wave reduction with different motion types for the FWBs.

In conclusion, floating-wetland breakwaters can reduce waves that cause erosion on the shorelines of lakes and reservoirs. This study determined that the wave height and energy density reduction performance of FWBs is comparable at different scales, therefore suggesting the ability to predict the wave reduction from FWBs of different sizes. This Master of Science thesis can serve as a first step in the study and implementation of FWBs as shoreline erosion mitigation technologies.

Chapter 7 - References

Allen H., 2001 Dec 27, Shoreline Erosion Control Plan, Lake Thunderbird, AllEnVironment Consulting.

Walker C., Tondera K., Lucke T. 2017. Stormwater Treatment Evaluation of a Constructed Floating Wetland after Two Years Operation in an Urban Catchment. Sustainability. 9(10):1687. doi:10.3390/su9101687.

Elhanafi A, et al. 2017. Scaling and air compressibility effects on a three-dimensional offshore stationary OWC wave energy converter. Applied Energy. 189:1–20. doi:10.1016/j.apenergy.2016.11.095.

Garcia Chance LM, White SA. 2018. Aeration and plant coverage influence floating treatment wetland remediation efficacy. Ecological Engineering. 122:62–68. doi:10.1016/j.ecoleng.2018.07.011.

Kinsman, B., 2002. Wind Waves: Their Generation and Propagation on the Ocean Surface. United States of America: Dover Publications.

Lynch J, et al. 2015. Evaluation of commercial floating treatment wetland technologies for nutrient remediation of stormwater. Ecological Engineering. 75:61–69. doi:10.1016/j.ecoleng.2014.11.001.

Mani, J. S., 1991, “Design of Y-frame floating breakwater.”J. Wtrwy., Port, Coast., and Oc. Engrg., ASCE, 117(2), 105–119

Martin Ecosystems., 2017 Jul 12, BioHaven Floating Wetland Technology White Paper, Martin Ecosystems.

Neelamani S, Ljubic J. “Experimental Study on the Hydrodynamic Performance of Floating Pontoon Type Breakwater With Skirt Walls.” Journal of Offshore Mechanics and Arctic Engineering, vol. 140, no. 2, 2018, pp. Journal of offshore mechanics and Arctic engineering, 2018–04-01, Vol.140 (2).

Pavlineri et al., 2017, Constructed floating wetlands: a review of research, design, operation and management aspects, and data meta-analysis, Chem. Eng., 308 (2017), pp. 1120-1132

Sayah et al., 2005, Field Measurements and Numerical Modelling of Wind-Waves in Lake Biel: A Basic Tool for Shore Protection Projects, Proceedings of the XXXI IAHR Congress, Seoul, Korea, 4332-4343.

Society NG, 2018 Mar 20, Erosion, National Geographic Society. [accessed 2019 Feb 22]. http://www.nationalgeographic.org/encyclopedia/erosion/.

Webb, Brett M., 2014 Mar 14, Wave transmission testing of the Martin Ecosystems BioHaven Floating Breakwater, Department of Civil Engineering, University of Alabama.

Thurman H. V., Trujillo A. P. (2001). Essentials of oceanography. Englewood Cliffs, N.J.: Prentice Hall.

LeMéhauté Bernard. (1976). An introduction to hydrodynamics and water waves. New York: Springer-Verlag.

Holthuijsen, Leo H. (2007). Waves in oceanic and coastal waters. Cambridge: Cambridge University Press.

Marani M., et al. (2011). Understanding and predicting wave erosion of marsh edges. Geophysical Research Letters, 38(21)

Laerd Statistics. One-way ANCOVA in SPSS Statistics. Retrieved June 09, 2020.

Williams, A.N, McDougal, W.G. “A Floating Pontoon Breakwater With a Wave Wall.” 2000.

Uzaki K., et al. (2016, October 11). Performance of the wave energy dissipation of a floating breakwater with truss structures and the quantification of transmission coefficients. Retrieved October 07, 2020.

Ozeren, Yavuz. “Experimental and Numerical Investigations of Floating Breakwater Performance.” The University of Mississippi, ProQuest Dissertations Publishing, 2009.

Angove C, et al. “Assessing the Efficiencies and Challenges for Nutrient Uptake by Aquatic Plants.” Journal of Experimental Marine Biology and Ecology, vol. 507, 2018, pp. 23–30.

Baldy V, et al. (2015) Experimental Assessment of the Water Quality Influence on the Phosphorus Uptake of an Invasive Aquatic Plant: Biological Responses throughout Its Phenological Stage. PLoS ONE 10(3): e0118844. doi:10.1371/journal.pone.0118844

Leonardi N., et al. (2016). A linear relationship between wave power and erosion determines salt-marsh resilience to violent storms and hurricanes. Proceedings of the National Academy of Sciences of the United States of America, 113(1), 64-68. Retrieved October 7, 2020.

Agency E. (2006, November 01). The rock manual: The use of rock in hydraulic engineering (2nd edition). Retrieved October 07, 2020.

Ozeren Y., & Wren, D. (2018). Wave Erosion of Cohesive and non-Cohesive Embankments: Laboratory Experiments. Retrieved October 7, 2020.

Stern F. (2013). Chapter 7 Dimensional Analysis and Modeling. Retrieved 2020.

Munson B. R. (2013). Fundamentals of fluid mechanics. Hoboken, N.J: Wiley.

Sadeghian A, et al. "Sedimentation and Erosion in Lake Diefenbaker, Canada: Solutions for Shoreline Retreat Monitoring." Environmental Monitoring and Assessment, vol. 189, no. 10, 2017, p. 507.

Hochstein A.B., Adams Jr, C.E. A Numerical Model of the Effects of Propeller Wash and Ship-Induced Waves from Commercial Navigation in an Extended Navigation Season on Erosion, Sedimentation, and Water Quality in the Great Lakes Connecting Channels and Harbors, 1986.

Jia H, et al. "Numerical Simulation of Hydrodynamic and Water Quality Effects of Shoreline Changes in Bohai Bay." Frontiers of Earth Science, vol. 12, no. 3, 2018, pp. 625–639.

Gabriel A.O., Bodensteiner, L.R. "Impacts of Riprap on Wetland Shorelines, Upper Winnebago Pool Lakes, Wisconsin." Wetlands, vol. 32, no. 1, 2012, pp. 105–117.